Volatile organic compound speciation above and within a Douglas Fir forest

Post-print of peer-reviewed article published by Elsevier.
Published article available at: http://dx.doi.org/10.1016/j.atmosenv.2014.04.035

Cite as:
Copeland, N., Cape, J. N., Nemitz, E., Heal, M. R., 2012. Volatile organic compound speciation above and within a Douglas Fir forest. *Atmospheric Environment* 94, 86-95.

Volatile organic compound speciation above and within a Douglas Fir forest

Nichola Copeland [1,2], J. Neil Cape [1], Eiko Nemitz [1], Mathew R. Heal [2]

[1] Centre for Ecology & Hydrology, Bush Estate, Penicuik, EH26 0QB, UK

[2] School of Chemistry, University of Edinburgh, West Mains Road, Edinburgh, EH9 3JJ, UK

Corresponding author:

Dr M. R. Heal (address as above)

Tel.: +44 (0)131 6504764

Email: m.heal@ed.ac.uk

Highlights

Concentrations and fluxes measured using PTR-MS with virtual disjunct eddy covariance

First non-terpenoid species fluxes and mixing ratios for Douglas fir canopy

Above-canopy emissions of monoterpenes comparable to previous studies of *P. menziesii*

Fluxes of several non-terpenoid VOCs were significant

Acetaldehyde, acetone & MTs elevated near bottom of canopy, MBO & estragole at top

Abstract

Mixing ratios and fluxes of volatile organic compounds (VOCs) were measured by PTR-MS (and GC-MS) and virtual disjunct eddy covariance during a three-week field campaign in summer 2009 within and above a Douglas fir (*Pseudotsuga menziesii*) forest in Speulderbos, the Netherlands. Measurements included the first non-terpenoid species fluxes and mixing ratios for Douglas fir canopy. Above-canopy emissions of monoterpenes were comparable to previous studies of *P. menziesii*, with standard emission factors for the first and second halves of the campaign of 0.8 ± 0.4 and 0.8 ± 0.3 μg g_{dw}^{-1} h^{-1}, and temperature coefficients of 0.19 ± 0.06 and 0.08 ± 0.05 $°C^{-1}$, respectively. Isoprene standard emission factors for the two halves of the campaign were 0.09 ± 0.12 and 0.16 ± 0.18 μg g_{dw}^{-1} h^{-1}. Fluxes of several non-terpenoid VOCs were significant, with maximum fluxes greater than has been measured for other coniferous species. α-Pinene was the dominant monoterpene within and above the canopy. Within canopy mixing ratios of individual species were generally greatest in early evening consistent with reduced vertical mixing and continued temperature-dependent emissions. Acetaldehyde, acetone and monoterpenes had elevated mixing ratios toward the bottom of the canopy (5-10 m) with assumed contribution from the large quantities of forest-floor leaf litter. MBO (2-methyl-3-buten-2-ol) and estragole had peak mixing ratios at the top of the canopy and are known to have coniferous sources. MVK + MACR (methyl vinyl ketone and methacrolein) also had highest mixing ratios at the top of the canopy consistent with formation from in-canopy oxidation of isoprene. The work highlights the importance of quantifying a wider variety of VOCs from biogenic sources than isoprene and monoterpenes.

Key words: BVOC, PTR-MS, vDEC, monoterpene, pinene, isoprene

1 Introduction

Emissions of volatile organic compounds (VOC) from vegetation are estimated as about 10 times greater globally than VOC emissions from anthropogenic sources (Guenther et al., 1995; Steiner and Goldstein, 2007). The dominant BVOC is isoprene (Guenther et al., 2006), estimated to contribute 44% of global BVOC emissions, with monoterpenes contributing 11%, and other VOCs comprising the remainder. The high atmospheric reactivity of many BVOC means such emissions have important regional impacts on atmospheric oxidising capacity, and on tropospheric ozone and secondary organic aerosol formation.

Coniferous forests are normally associated with monoterpene emissions and low (or zero) isoprene emissions (Geron et al., 2000; Karl et al., 2009). Douglas fir is reported to be within the top 10 monoterpene-emitting tree species in the USA (Geron et al., 2000) but previous studies on Douglas fir have investigated emissions at the leaf and branch scale. Arey et al. (1995) measured a standardised monoterpene emission rate (at 30 °C and 1000 μmol m^{-2} s^{-1}) of 1.1 μg g_{dw}^{-1} h^{-1} for bigcone Douglas fir (*Pseudotsuga macrocarpa*), with α-pinene and limonene as major components, and β-pinene and 3-carene also detected. An emission rate of 0.44 μg g_{dw}^{-1} h^{-1} was reported for coastal Douglas fir (*Pseudotsuga menziesii*) (Pressley et al., 2004). The highest reported standardised monoterpene emission rate is 2.60 μg g_{dw}^{-1} h^{-1} from *Pseudotsuga menziesii* (Drewitt et al., 1998). An isoprene emission rate of 1.72 μg g_{dw}^{-1} h^{-1} was also reported. A study which investigated a wider range of VOC emissions from saplings also detected sesquiterpenes, oxygenated terpene products (including 2-methyl-3-buten-2-ol (MBO)), methyl salicylate and a homoterpene ($C_{11}H_{18}$) (Joó et al., 2011).

Quantification of VOC emissions from Douglas fir warrants further research due to paucity of data at canopy scale and for non-terpenoid compounds, and the variability in previously reported standard emissions. In this work, fluxes and mixing ratios of VOCs were measured above and within a Douglas fir canopy at Speulderbos, the Netherlands. A previous study at this site measured forest floor and above-canopy mixing ratios of α-pinene, β-pinene, 3-carene and limonene (Dorsey et al., 2004). Monoterpene mixing ratios above the forest floor were greater than those measured above-canopy, which was attributed to leaf litter emissions, and were also greatest at night because of the lower atmospheric mixing. These findings broadly corroborated those of an earlier study (Peters et al., 1994). However, neither of these studies measured fluxes or other VOC species.

2 Methods

2.1 Sampling site

Measurements were made from 15 June to 10 July 2009 at an established site in Speulderbos forest near Garderen, Netherlands (52º 15′ N, 5º 41′ E, 50 m asl, Supplementary information Figure S1), operated by RIVM (Rijksinstituut voor Volksgezondheid en Milieu). The forest comprises a dense monoculture of mature Douglas fir (*Pseudotsuga menziesii*, ~2.3 ha, Figure S2), planted in 1960, within a larger forested area (50 km^2). The soil is an orthic podzol/holtpodzol with loamy sand texture. The maximum canopy height was ~32 m. Due to the high planting density there was almost no tree foliage below 8 m and little light penetration to the forest floor.

The nearest settlements to the site are Garderen (2.5 km SE, population ~2,000), Putten (5.7 km WNW, population ~23,000) and Ermelo (6.6 km NW, population ~26,000), while the

nearest major city is Apeldoorn (19 km ESE, population ~156,000). There was very little traffic on surrounding roads.

Flux footprints for the sampling location were predicted with a simple parameterisation model (Kljun et al., 2004) using minimum, maximum and mean u^* values (Figure S3). The largest distance which encompassed 80% of the flux contribution at the monitoring site across the range of friction velocities encountered during the campaign was 660 m. This distance was within a uniform area of forest for all wind directions (Figure S4).

2.2 PTR-MS set-up

BVOC mixing ratios and fluxes above the forest canopy were measured using proton transfer reaction mass spectrometry (PTR-MS) (Blake et al., 2009) coupled with virtual disjunct eddy covariance (vDEC) (Karl et al., 2002; Rinne et al., 2001). The PTR-MS instrument (Ionicon Analytik, Innsbruck, Austria) was fitted with an extra turbopump connected to the detection chamber, and Teflon instead of Viton rings in the drift tube (Copeland et al., 2012; Misztal et al., 2010). Pfeiffer turbopumps replaced the Varian equivalents. Drift tube conditions were held constant throughout (pressure 1.7 mbar, temperature 45 °C, voltage 478 V) to maintain an E/N ratio of ~130 Td (1 Td = 10^{-17} V cm^2).

The sampling inlet and 20 Hz sonic anemometer (WindmasterPro, Gill Instruments) were positioned above the canopy at the top of a 45 m tower. Air was sampled at 23.5 L min^{-1} through a 50 m PTFE inlet line (1/4″ OD, 3/16″ ID) with a T-piece for sub-sampling into the PTR-MS inlet at a rate of 250 mL min^{-1}. Condensation of water vapour in the inlet line was prevented by wrapping with self-regulating heating tape (Omega, UK type SRF3-2C). Data were logged using a program written in LabVIEW (Version 8.5, National Instruments).

2.3 Determination of VOC mixing ratios and fluxes

The PTR-MS signal was calibrated explicitly for several VOCs using a mixed-gas calibration cylinder (Apel-Riemer Environmental Inc., USA) containing 1 ppmv each of formaldehyde, methanol, acetonitrile, acetone, acetaldehyde, isoprene and 0.18 ppmv d-limonene. The calibration gas was diluted with VOC-scrubbed air to produce 6 samples with concentrations of 0.5, 1.0, 10, 20, 30 and 50% of the pure calibration gas standard. A relative transmission curve was constructed to determine empirical calibration coefficients for other VOCs under study not present in the standard (Taipale et al., 2008). Calibrations were carried out in the lab before commencement of the field campaign, and on 8 July during the campaign. Limits of detection (LOD) were calculated as twice the standard deviation of the background ion counts for a particular *m/z* divided by sensitivity (ncps $ppbv^{-1}$) (Karl et al., 2003). Detailed information on cross-check of the PTR-MS calibration is given in the supplementary material of Misztal et al. (2011).

For the first 10 days of measurements (18-28 June) the PTR-MS operated in multiple ion detection (MID) mode for two 25 min periods per hour. During these periods only the targeted VOC ions listed in Table 1 were measured (0.5 s dwell times), in addition to the primary ion H_3O^+, and water cluster $(H_2O)H_3O^+$ (0.2 s dwell times). This gave a sampling cycle time over the 14 target *m*/*z* values in Table 1 of 6.4 s, with each of the organic target masses sampled for 0.5 s in each cycle. Sensitivities and LODs for target ions are given in Table 1. The remaining 10 min per hour was used for full mass scans in the range 21–206 amu at a dwell time of 1 s per amu. For one 5 min period, ambient air was scanned to allow information about full VOC composition to be acquired. For a further 5 min per hour, 'zero air' was scanned to determine instrument background. Zero air was achieved by sampling

ambient air through a zero-air generator comprising a glass tube packed with platinum wool and a 50:50 mixture of platinum mesh and activated charcoal heated to 200 °C. The background spectrum was subtracted in subsequent data processing.

As the PTR-MS was run in MID mode, fewer data points were generated than required for direct eddy covariance due to the non-continuous manner in which the quadrupole mass analyser measures each *m/z*. The set-up resulted in 30,000 wind speed measurements and up to 203 VOC measurements in each 25 min sampling period. The lag time between PTR-MS and wind speed data due to residence time in the sampling inlet line and disjunction between sonic and PTR-MS data was determined by finding the maximum in cross-correlation between vertical wind speed and VOC mixing ratio as a function of lag time (with 15 s window). A program written in LabVIEW was used to determine lag times separately for each compound within each 25 min flux sampling period. Mean lag times were in the range 6.5 to 7.1 s. This includes an estimated transition time of 2.3 s between the sampling point and analyser input; the remainder resulted from delays in the data-handling software.

Quality control criteria were applied to filter data for periods of low friction velocity (u^* <0.15 m s^{-1}), non-stationarity, large spikes in vertical wind speed or VOC concentration, and where <10,000 data points (5.5 % of all data) were acquired in a 25 min sampling period. Most discarded data occurred during night when turbulence was low (48.3% of all data points). High-frequency flux losses due to relatively slow disjunct VOC sampling frequency (2 Hz, compared to 20 Hz sonic data capture) were estimated using empirical ogive analysis (Ammann et al., 2006) for each 25 min period and flux values corrected accordingly. Standard rotations of the coordinate frame were applied to correct for sonic anemometer tilt for each 25 min period separately.

2.4 In-canopy measurements

From 30 June to 7 July in-canopy mixing ratios were also measured. A pulley system allowed continuous movement of the PTR-MS inlet between heights of 4 and 32 m. During this period, above-canopy measurements were taken during the first half of every hour (hh:05 to hh:30) and in-canopy measurements were taken in the latter half of every hour (hh:35 to hh:00). Full mass scans of ambient air and zero air were taken for 5 min intervals at hh:00 and hh:30 respectively. PAR and temperature were also measured from the gradient system.

2.5 Chromatographic analysis of ambient air samples

Ambient air samples were collected above the canopy on 6 July 2009 for subsequent GC-MS analysis. Samples were also taken at heights of 32, 18 and 4 m three times during the day on 1 and 6 July 2009. The collection of these samples was for spot inter-comparison against the continuous PTR-MS data, and to provide an indication of speciation between α-pinene and β-pinene, which the PTR-MS cannot distinguish. Given the limited dataset from these measurements, the detail of the methods and results are presented in the Supplementary Information, with key observations highlighted here.

3 Results

3.1 Above canopy fluxes

The full time series of above-canopy VOC fluxes along with u^* and sensible heat flux are shown in Figure S5. Two periods of missing data 25-26 June and 3 July were due to problems with a data communication cable and the sampling pump, respectively. Most missing data at night were due to exclusion of low u^* values. The winch set-up commenced 29 June at 20:00,

after which above-canopy data were hourly rather than half-hourly. Because of the difference in measurement frequency, data from the two halves of the campaign were treated separately. Diurnal profiles of VOC fluxes for the first half are shown in Figure 1. Since raw flux data were relatively noisy, median values were calculated for each half-hourly time step and the 3-hour running mean plotted e.g. the data point plotted for 12:00 is the mean of median values from 10:30 to 13:30.

Positive daytime fluxes were discernible for acetaldehyde, acetone and monoterpenes, with near-zero or depositional fluxes at night following the sharp decrease in sensible heat flux. (Note that the term 'zero' here should be interpreted in the context of the variability in values encapsulated by the grey shading of Figure 1.) Diurnal trends in methanol and isoprene fluxes were similar, with minima (~ –0.8 and ~ –0.15 mg m^{-2} h^{-1}, respectively) during the day and maxima (~0.5 and ~0.2 mg m^{-2} h^{-1}, respectively) in the evening or at night. This was particularly pronounced for isoprene, which had a sharp increase in emission to its maximum between 12:00 and 18:00, coinciding with maximum PAR, before decreasing rapidly to zero towards sunset. The diurnal pattern of isoprene oxidation products MVK + MACR fluctuated throughout the day with small positive fluxes in the morning and early evening, when isoprene emissions declined but isoprene photo-oxidation continued.

Fluxes of hexanals and MBO were near-zero except for some positive fluxes between 18:00 and 00:00. Conversely, TMA, *p*-cymene and estragole had negative fluxes in the evening, with TMA and *p*-cymene fluxes around zero for the remainder of the day and estragole having positive fluxes overnight. However, the majority of these fluxes were below LOD.

There was a discrepancy in monoterpene fluxes determined from *m/z* 81 and *m/z* 137 ions with the latter yielding greater values. The inconsistency may be due to differences in fragmentation patterns between monoterpenes, as has been observed in other studies (Rinne et al., 2007). Measurements for MT137 were also below LOD so determinations at MT81 are likely more reliable.

Diurnal profiles were noisier for the second half of the campaign because of the less frequent sampling (Figure S6). Absolute fluxes tended to be greater during the second half, as were temperatures. Daily patterns showed some similarities to those in the first half but were less distinct.

3.2 Above-canopy mixing ratios

The full time series of above-canopy mixing ratios and temperature are shown in Figure S7. Average diurnal profiles of VOC mixing ratios for the first half of the campaign are shown in Figure 2. All compounds, except *p*-cymene, had similar daily patterns of minima around midday and maxima at night. Amplitudes of diurnal cycle were small for most compounds, with those for methanol, acetaldehyde and acetone being most pronounced. *p*-Cymene had a relatively constant mixing ratio for most of the day but was elevated from mid-morning to mid-afternoon. Hexanals, MBO, *p*-cymene, MT137 and estragole mixing ratios were below calculated LOD, although all showed discernible daily patterns within a narrow variability band, and have therefore been presented. It is possible that the reliability of removal of the compounds was not consistent, resulting in high LOD. Diurnal profiles of VOC mixing ratios for the second half of the campaign (Figure S8) were lower than during the first half and showed similar diurnal trends. Within the limitations of the methodology described in the Supplementary Information, the GC-MS measurements showed general consistency in the

daily pattern and magnitude of mixing ratios for the pinenes (Figure S10) with those determined by PTR-MS.

3.2.1 Wind direction/speed trends

To aid identification of geographic origins of potential VOC sources, Figure S9 shows bivariate polar plots of VOC mixing ratio as a function of wind speed and direction, combining data from both halves of the campaign. The bivariate plots for most compounds were similar, with greater mixing ratios when the wind was from S or NE, particularly for high wind speeds (suggesting contributions from distant sources). Additionally, more localised sources from the S, when wind speeds were lower, were particularly evident for acetone, and for all other compounds. With the exception of acetaldehyde, acetone and methanol, mixing ratios were also elevated for the NW wind direction, coinciding with higher air temperatures. Greatest mixing ratios of *p*-cymene were observed for winds from the NW, the only compound with a bivariate pattern notably different to all others.

Forest surrounds the site for several km in all directions except for a large expanse of heather 1.5 km to the E. The nearest sizable urban area is 6 km NW near Ermelo and Putten. On a wider scale, Speuld lies within an area of land mostly covered by deciduous forest and natural vegetation (Figure S1) extending 50 km N-S and covering an area of ~870 km^2 (Clevers et al., 2007). Outside the wider forested area, a large area of agricultural land covering most of the Flevopolder region (970 km^2) lies 15 km NW. Amsterdam is ~55 km WNW. At a horizontal wind speed of 2 m s^{-1} it would take less than 8 h to travel this distance, which is much shorter than some of the typical atmospheric lifetimes of measured compounds, including methanol, acetaldehyde, acetone, TMA and MVK (as summarised in Table S1).

It is likely that the tendency for high mixing ratios in N and S directions is due to the wider forested area, as this is the most dominant land use in these directions. Of compounds also showing high mixing ratios from the NW sector, TMA and hexanals have lifetimes of the order of several hours, therefore the Flevopolder region may be a source of these compounds. Animal husbandry is cited as the main source of atmospheric TMA (Ge et al., 2011) with slurry application a minor contributor (Kuhn et al., 2011), and hexanals are known to be emitted during grass cutting (Davison et al., 2008; Karl et al., 2005b).

Greater *p*-cymene mixing ratios from the NW may also be due to these sources, although *p*-cymene emission is more commonly associated with deciduous broadleaf forests (Geron et al., 2000). Alternatively, as *p*-cymene is detected at the same *m*/*z* as toluene (normally from anthropogenic sources), it may be possible that it is the latter which was detected. Possible sources could have been urban centres such as Putten/Ermelo or, further afield, Amsterdam, which is feasible for this compound's relatively long lifetime (2.4 day for 1.5×10^{6} cm^{-3} OH).

3.3 In-canopy mixing ratios

Plots visualising the within-canopy vertical variation in the mixing ratios determined by PTR-MS, as a function of time of day, are shown in Figure 3. Mixing ratios were generally higher than those measured above-canopy (Figures 2 and S8). All compounds displayed similar diurnal patterns to those observed for above-canopy measurements, with mixing ratios increasing throughout the second half of the day. Maxima were at ~18:00, corresponding to reduced vertical mixing and continued temperature-dependant emissions.

Methanol, acetaldehyde, acetone, isoprene, monoterpenes and hexanals exhibited peak mixing ratios within the canopy at ~18:00, with distinct minima around 06:00 for all except

monoterpenes (minimum ~13:00). Isoprene mixing ratios decreased more rapidly than for other compounds, reaching the minimum by midnight. Acetaldehyde, acetone and monoterpenes had particularly elevated mixing ratios toward the bottom of the canopy (5-10 m), as had been observed for monoterpenes during previous work (Dorsey et al., 2004). This may be due to large quantities of leaf litter on the forest floor acting as a source.

MVK + MACR, MBO and estragole had peak mixing ratios at the top of the canopy. For MVK + MACR this can be explained by formation in-canopy from oxidation of isoprene, rather than primary emission, therefore peak mixing ratio coincides with highest PAR at the top of the canopy. Pine species are reported a source of MBO (Harley et al., 1998) with emission dependant on both light and temperature (Holzinger et al., 2005). Estragole emission occurs via both storage pools (similar to monoterpenes) and directly after synthesis in a light and temperature driven mechanism (similar to MBO) (Bouvier-Brown et al., 2009). Increased PAR higher in the canopy may therefore explain mixing ratio profiles of these compounds, while storage pool emissions of estragole result in a slower decline in mixing ratios overnight.

TMA and *p*-cymene profiles differed from all others and were less structured. TMA mixing ratios were, in general, greater towards the top of the canopy, except for ~18:00 when mixing ratios were elevated at all heights. Mixing ratios also remained high overnight. Peak *p*-cymene mixing ratios were between 22:00 and 06:00 low in the canopy (5-10 m).

The GC-MS data presented in the Supplementary Information support the observations from the in-canopy PTR-MS measurements that total measured monoterpene mixing ratios (comprising α- and β-pinene, 3-carene and limonene) were generally larger at lower heights (Figure S11), similar to a previous study at the Speuld site (Peters et al., 1994). In-canopy (4

and 18 m) mixing ratios were highest in the morning and evening and lowest in the afternoon, with largest afternoon mixing ratios at the top of the canopy (32 m) and above (40 m). The four measured monoterpenes are consistent with Lerdau et al. (1995) who reported that α-pinene, β-pinene and 3-carene account for 95 % monoterpene emissions from Douglas fir. α-Pinene is the dominant monoterpene at all heights within and above the canopy (Figure S12).

4 Discussion

4.1 Terpenoids

Monoterpene mixing ratios observed in this work are in agreement with previous observations at the site (Dorsey et al., 2004; Peters et al., 1994). They were generally larger at night, peaking at 23:30 (1.76 ppbv) and 16:00 (0.95 ppbv) during the first and second halves of the campaign, respectively, and larger closer to the forest floor, suggesting a source contribution low in the canopy such as the large quantities of leaf litter.

Monoterpene fluxes from vegetation have been shown to increase exponentially with temperature (Guenther et al., 1993; Pressley et al., 2004), according to the G93 algorithm,

$$E_{meas} = E_s e^{[\beta(T - T_s)]} \quad (1)$$

where E_{meas} is measured emission rate at leaf temperature T (°C), E_s is the standard emission rate at 30 °C (T_s) and β is an empirical temperature coefficient. To convert from an area flux to a foliar mass flux a foliar density D of 600 g_{dw} m^{-2} was assumed for *Pseudotsuga spp*. (Guenther et al., 1994). See below for comment on uncertainty in this value. The canopy temperature was not directly measured so a sensitivity of the derived standardised monoterpene flux to this temperature parameter was undertaken. Using Equation (1) and above-canopy temperature the standard monoterpene emission rates for the two halves of the

campaign were calculated to be 1.0 ± 0.5 and 0.9 ± 0.2 μg g_{dw}^{-1} h^{-1}, with temperature coefficients of 0.19 ± 0.06 and 0.08 ± 0.05 $°C^{-1}$, respectively. For these measurements in temperate latitudes it is anticipated that the canopy temperature is in the range around 2 K higher than the above-canopy temperature, which decreases the derived standardised emission rates to 0.8 ± 0.3 and 0.8 ± 0.2 μg g_{dw}^{-1} h^{-1} for the two halves of the campaign, respectively. (Same temperature coefficients.) These latter standardised monoterpene fluxes are well within the uncertainties of the previously-calculated standardised fluxes but because of the systematic nature of the effect of temperature these latter fluxes are taken as the better estimates. Realistic levels of uncertainty in the temperature parameter will not alter the calculated emission rates outside of the large uncertainty ranges that are already associated with deriving these values from the measurement data.

Uncertainty in the value of *D* contributes further uncertainty to the derived emission rates. Anticipating that relative uncertainty in *D* is within 20% modifies the statistical uncertainty ranges for the standard MT emission rates in the two halves of the campaign to 0.8 ± 0.4 and 0.8 ± 0.3 μg g_{dw}^{-1} h^{-1}. The standardised values are compared with other Douglas fir studies in Table 2. The large statistical standard deviations in the derived parameters reflect the scatter in the relationships between E_{meas} and *T* observed in this work (R^2 = 0.29 and 0.17 for the first and second halves of the campaign, respectively), which is likely due to noisy flux data and being close to instrument LOD. The second half of the campaign also has only half the number of above-canopy flux data because of the interspersed in-canopy measurements. The standard monoterpene emission factors from this study are within the range of previously derived values for *P. menziesii*. All other studies used branch enclosure methods. Short-duration temperature and light differences within the canopy would lead to deviations of canopy-scale averages from enclosure studies. The temperature coefficients derived from the

two halves of the study although differing by more than a factor of two are not statistically significant different because of the large uncertainties, and are in line with the generally accepted value for most plants (Guenther et al., 1993).

Although Douglas fir trees – and coniferous species in general – are thought to be non-emitters of isoprene, fluxes were discernible, as they were for isoprene oxidation products MVK + MACR. The above-canopy mixing ratios of these species exhibited a diurnal pattern throughout the campaign. Figure 3 shows that elevated isoprene mixing ratios occurred throughout the canopy, whilst maximum MVK + MACR mixing ratios were at the top of the canopy, ~32 m. This supports the forest canopy as a source of isoprene, which is oxidised to form MVK and MACR, peaking at the canopy top where PAR is greatest. As isoprene emission from plants is strongly influenced by light and temperature, the canopy-level emission, F, was recalculated as a standard emission factor (ε) for a leaf temperature of 303 K and PAR flux of 1000 μmol m^{-2} s^{-1}, as described by the G95 algorithm (Guenther et al., 1995),

$$\varepsilon = \frac{F}{D\,\gamma} \tag{2}$$

where D is foliar density (g_{dw} m^{-2}) and γ is a non-dimensional activity adjustment factor to account for effects of light and temperature:

$$\gamma = C_L C_T \tag{3}$$

The light dependence, C_L, is defined by

$$C_L = \frac{\alpha c_{L1} Q}{\sqrt{1+\alpha^2 Q^2}} \tag{4}$$

where α (0.0027) and c_{L1} (1.066) are empirical coefficients and Q is PAR flux (μmol m^{-2} s^{-1}). The temperature dependence C_T, is defined by

$$C_T = \frac{exp\frac{c_{T1}(T-T_S)}{RT_ST}}{1+exp\frac{\left(c_{T2}(T-T_M)\right)}{RT_ST}} \quad (5)$$

where T is leaf temperature (K), T_s is leaf temperature at standard conditions (303 K), R is the universal gas constant (8.314 J K^{-1} mol^{-1}), and c_{T1} (95 kJ mol^{-1}), c_{T2} (230 kJ mol^{-1}) and T_M (314 K) are empirical coefficients.

Hourly values of above-canopy PAR and temperature, and of isoprene flux (from Figures 1 and S6), were used to calculate γ and F respectively. As above, a 2 K enhancement of ambient temperature was assumed as a better proxy of canopy temperature, and also as above a foliar density of 600 g_{dw} m^{-2} was used. Hourly emission factors ε were then determined for isoprene for the first and second halves of the campaign, and these had peak values of 0.64 and 0.62 µg g_{dw}^{-1} h^{-1}, respectively. Mean daytime standard values of 0.09 ± 0.12 and 0.16 ± 0.18 µg g_{dw}^{-1} h^{-1} were calculated to allow comparison in Table 2 with mean values from other studies. These flux values are also subject to uncertainty from the assumed foliar density which we anticipate should be within 20%. Standard isoprene emission factors from this study were at the low end previously derived values for *Pseudotsuga spp*., but the values here are canopy scale rather than branch scale and variability quoted in all measurements is large.

4.2 Non-terpenoids

Non-terpenoids were investigated for the first time at the Speuld site. Only one previous study could be found which qualitatively measured other VOCs from Douglas fir saplings (Joó et al., 2011). Positive fluxes were observed for all compounds determined except TMA and *p*-cymene (and/or toluene) which exhibited net deposition. Maximum daily median fluxes of some oxygenated compounds were larger than from other coniferous studies. Methanol and acetaldehyde fluxes (2.6 and 0.7 mg m^{-2} h^{-1}, respectively (Figure S6) were larger than those

measured in a subalpine, coniferous forest in USA where fluxes peaked at 1 and 0.4 mg m^{-2} h^{-1}, respectively (Karl et al., 2002). Acetone fluxes were identical at both sites (0.8 mg m^{-2} h^{-1}). Methanol, acetaldehyde and acetone fluxes at Speuld were also higher than those above a Scots pine canopy in Finland (0.4, 0.15 and 0.3 mg m^{-2} h^{-1}, respectively (Rinne et al., 2007)). In both studies, measurements were carried out during summer (June and July, respectively). Daily temperatures at the subalpine site in USA peaked at ~17 °C. In contrast, peak temperatures at the Finnish site were only slightly cooler (~25 °C) than at Speuld but night-time minimum temperatures were much cooler (~14 °C). Higher temperatures at Speuld may therefore account for the larger measured fluxes here than at these other locations.

In-canopy mixing ratios further support Douglas fir as a source of methanol, acetaldehyde, acetone, hexanals, MBO and estragole. It has been shown in several studies that decaying plant material is a source of oxygenated VOCs, such as ponderosa pine (Schade and Goldstein, 2001), loblolly pine (Karl et al., 2005a) and decaying spruce needles (Warneke et al., 1999). As there was a thick layer of leaf litter on the forest floor, it is feasible that this was a source of oxygenated VOCs, particularly acetaldehyde and acetone which had highest mixing ratios near the forest floor.

Above-canopy mixing ratios of all VOCs followed a similar diurnal trend of maxima in the evening or at night, with methanol, acetaldehyde, acetone, TMA, isoprene and MVK + MACR all above LOD. This can be explained by reduced radical sink chemistry at night, coupled with reduced vertical mixing, resulting in accumulation within a shallower boundary layer.

Mixing ratios of all compounds appeared to be predominantly influenced by the wider forested area, with more distant sources also identified, particularly for TMA and *p*-cymene. Arable and grass land NW of the site was thought to be a source of elevated TMA mixing ratios. Elevated mixing ratios at *m*/*z* 93 were potentially attributable to anthropogenic toluene, as evidenced from Figure S9 which shows elevated mixing ratios associated with urban areas in the WNW direction. These PTR-MS measurements were unable to discriminate different compounds with identical *m*/*z*.

5 Conclusions

Fluxes and mixing ratios of VOC were measured by PTR-MS and vDEC at a Douglas fir forest in Speuld, The Netherlands. Monoterpene fluxes were comparable with other studies of Douglas fir, with calculated standard emission factor of 0.8 ± 0.4 and 0.8 ± 0.3 μg g_{dw}^{-1} h^{-1}, and temperature coefficients of 0.19 ± 0.06 and 0.08 ± 0.05 $°C^{-1}$ for the first and second halves of the campaign, respectively. Mean standard emission factors for isoprene were 0.09 ± 0.12 and 0.16 ± 0.18 μg g_{dw}^{-1} h^{-1} for the two halves respectively.

Fluxes of several non-terpenoid VOCs were significant, with maximum fluxes greater than has been measured for other coniferous species. α-Pinene was the dominant monoterpene within and above the canopy. Within canopy mixing ratios of individual species were generally greatest in early evening consistent with reduced vertical mixing and continued temperature-dependent emissions. Acetaldehyde, acetone and monoterpenes had elevated mixing ratios toward the bottom of the canopy (5-10 m) with likely contribution from the large quantities of forest-floor leaf litter. MBO and estragole had peak mixing ratios at the top of the canopy and are known to have coniferous sources. MVK + MACR also had highest mixing ratios at the top of the canopy consistent with formation from in-canopy oxidation of

isoprene. The work highlights the importance of quantifying a wider variety of VOCs from biogenic sources than isoprene and monoterpenes.

Acknowledgements

N. Copeland acknowledges PhD studentship funding from the University of Edinburgh School of Chemistry and CEH Edinburgh. These measurements were collected as part of a fieldwork campaign within the EU NitroEurope programme. The authors thank: Arnoud Frumau (ECN) and Hilbrand Westrate (TNO) for site access; Chiara di Marco, Pawel Misztal, Eiko Nemitz, Gavin Phillips (all CEH Edinburgh), Max McGillan and Paul Williams (University of Manchester) for site and instrument set up; and Amy Tavendale for in-canopy data presentation.

References

Ammann, C., Brunner, A., Spirig, C., Neftel, A., 2006. Technical note: Water vapour concentration and flux measurements with PTR-MS. Atmospheric Chemistry and Physics 6, 4643-4651.

Arey, J., Crowley, D. E., Crowley, M., Resketo, M., Lester, J., 1995. Hydrocarbon Emissions from Natural Vegetation in California South-Coast-Air-Basin. Atmospheric Environment 29, 2977-2988.

Blake, R. S., Monks, P. S., Ellis, A. M., 2009. Proton-Transfer Reaction Mass Spectrometry. Chemical Reviews 109, 861-896.

Bouvier-Brown, N. C., Goldstein, A. H., Worton, D. R., Matross, D. M., Gilman, J. B., Kuster, W. C., Welsh-Bon, D., Warneke, C., de Gouw, J. A., Cahill, T. M., Holzinger, R., 2009. Methyl chavicol: characterization of its biogenic emission rate, abundance, and oxidation products in the atmosphere. Atmospheric Chemistry and Physics 9, 2061-2074.

Clevers, J., Schaepman, M., Mucher, C., De Wit, A., Zurita-Milla, R., Bartholomeus, H., 2007. Using MERIS on Envisat for land cover mapping in the Netherlands. International Journal of Remote Sensing 28, 637-652.

Copeland, N., Cape, J. N., Heal, M. R., 2012. Volatile organic compound emissions from *Miscanthus* and short rotation coppice willow bioenergy crops. Atmospheric Environment 60, 327-335.

Davison, B., Brunner, A., Ammann, C., Spirig, C., Jocher, M., Neftel, A., 2008. Cut-induced VOC emissions from agricultural grasslands. Plant Biology 10, 76-85.

Dorsey, J. R., Duyzer, J. H., Gallagher, M. W., Coe, H., Pilegaard, K., Weststrate, J. H., Jensen, N. O., Walton, S., 2004. Oxidized nitrogen and ozone interaction with forests. I: Experimental observations and analysis of exchange with Douglas fir. Quarterly Journal of the Royal Meteorological Society 130, 1941-1955.

Drewitt, G. B., Curren, K., Steyn, D. G., Gillespie, T. J., Niki, H., 1998. Measurement of biogenic hydrocarbon emissions from vegetation in the lower Fraser valley, British Columbia. Atmospheric Environment 32, 3457-3466.

Ge, X., Wexler, A. S., Clegg, S. L., 2011. Atmospheric amines - Part I. A review. Atmospheric Environment 45, 524-546.

Geron, C., Rasmussen, R., Arnts, R. R., Guenther, A., 2000. A review and synthesis of monoterpene speciation from forests in the United States. Atmospheric Environment 34, 1761-1781.

Guenther, A., Hewitt, C. N., Erickson, D., et al , 1995. A global model of natural volatile organic compound emissions. Journal of Geophysical Research 100, 8873-8892.

Guenther, A., Karl, T., Harley, P., Wiedinmyer, C., Palmer, P. I., Geron, C., 2006. Estimates of global terrestrial isoprene emissions using MEGAN (Model of Emissions of Gases and Aerosols from Nature). Atmospheric Chemistry and Physics 6, 3181-3210.

Guenther, A., Zimmerman, P., Wildermuth, M., 1994. Natural Volatile Organic-Compound Emission Rate Estimates for United-States Woodland Landscapes. Atmospheric Environment 28, 1197-1210.

Guenther, A. B., Zimmerman, P. R., Harley, P. C., Monson, R. K., Fall, R., 1993. Isoprene and Monoterpene Emission Rate Variability - Model Evaluations and Sensitivity Analyses. Journal of Geophysical Research 98, 12609-12617.

Harley, P., Fridd-Stroud, V., Greenberg, J., Guenther, A., Vasconcellos, P., 1998. Emission of 2-methyl-3-buten-2-ol by pines: A potentially large natural source of reactive carbon to the atmosphere. Journal of Geophysical Research-Atmospheres 103, 25479-25486.

Holzinger, R., Lee, A., Paw, K. T., Goldstein, A. H., 2005. Observations of oxidation products above a forest imply biogenic emissions of very reactive compounds. Atmospheric Chemistry and Physics 5, 67-75.

Joó, E., Dewulf, J., Amelynck, C., Schoon, N., Pokorska, O., Simpraga, M., Steppe, K., Aubinet, M., Van Langenhove, H., 2011. Constitutive versus heat and biotic stress induced BVOC emissions in *Pseudotsuga menziesii*. Atmospheric Environment 45, 3655-3662.

Karl, M., Guenther, A., Koble, R., Leip, A., Seufert, G., 2009. A new European plant-specific emission inventory of biogenic volatile organic compounds for use in atmospheric transport models. Biogeosciences 6, 1059-1087.

Karl, T., Hansel, A., Mark, T., Lindinger, W., Hoffmann, D., 2003. Trace gas monitoring at the Mauna Loa Baseline observatory using proton-transfer reaction mass spectrometry. International Journal of Mass Spectrometry 223, 527-538.

Karl, T., Harley, P., Guenther, A., Rasmussen, R., Baker, B., Jardine, K., Nemitz, E., 2005a. The bi-directional exchange of oxygenated VOCs between a loblolly pine (*Pinus taeda*) plantation and the atmosphere. Atmospheric Chemistry and Physics 5, 3015-3031.

Karl, T., Harren, F., Warneke, C., de Gouw, J., Grayless, C., Fall, R., 2005b. Senescing grass crops as regional sources of reactive volatile organic compounds. Journal of Geophysical Research-Atmospheres 110, D15302, doi:10.1029/2005JD005777 .

Karl, T. G., Spirig, C., Rinne, J., Stroud, C., Prevost, P., Greenberg, J., Fall, R., Guenther, A., 2002. Virtual disjunct eddy covariance measurements of organic compound fluxes from a subalpine forest using proton transfer reaction mass spectrometry. Atmospheric Chemistry and Physics 2, 279-291.

Kesselmeier, J., Staudt, M., 1999. Biogenic volatile organic compounds (VOC): An overview on emission, physiology and ecology. Journal of Atmospheric Chemistry 33, 23-88.

Kljun, N., Calanca, P., Rotachhi, M. W., Schmid, H. P., 2004. A simple parameterisation for flux footprint predictions. Boundary-Layer Meteorology 112, 503-523.

Kuhn, U., Sintermann, J., Spirig, C., Jocher, M., Ammann, C., Neftel, A., 2011. Basic biogenic aerosol precursors: Agricultural source attribution of volatile amines revised. Geophysical Research Letters 38, L16811, doi:10.1029/2011GL047958.

Lerdau, M., Matson, P., Fall, R., Monson, R., 1995. Ecological Controls Over Monoterpene Emissions from Douglas-Fir (*Pseudotsuga-Menziesii*). Ecology 76, 2640-2647.

Misztal, P. K., Nemitz, E., Langford, B., Di Marco, C. F., Phillips, G. J., Hewitt, C. N., MacKenzie, A. R., Owen, S. M., Fowler, D., Heal, M. R., Cape, J. N., 2011. Direct ecosystem fluxes of volatile organic compounds from oil palms in South-East Asia. Atmospheric Chemistry and Physics 11, 8995-9017.

Misztal, P. K., Owen, S. M., Guenther, A. B., Rasmussen, R., Geron, C., Harley, P., Phillips, G. J., Ryan, A., Edwards, D. P., Hewitt, C. N., Nemitz, E., Siong, J., Heal, M. R., Cape, J. N., 2010. Large estragole fluxes from oil palms in Borneo. Atmospheric Chemistry and Physics 10, 4343-4358, doi:10.5194/acp-10-4343-2010.

Peters, R. J. B., Duivenbode, J. A. D. V., Duyzer, J. H., Verhagen, H. L. M., 1994. The determination of terpenes in foreset air. Atmospheric Environment 28, 2413-2419.

Pressley, S., Lamb, B., Westberg, H., Guenther, A., Chen, J., Allwine, E., 2004. Monoterpene emissions from a Pacific Northwest Old-Growth Forest and impact on regional biogenic VOC emission estimates. Atmospheric Environment 38, 3089-3098.

Rinne, H. J. I., Guenther, A. B., Warneke, C., de Gouw, J. A., Luxembourg, S. L., 2001. Disjunct eddy covariance technique for trace gas flux measurements. Geophysical Research Letters 28, 3139-3142.

Rinne, J., Taipale, R., Markkanen, T., Ruuskanen, T., Hellen, H., Kajos, M., Vesala, T., Kulmala, M., 2007. Hydrocarbon fluxes above a Scots pine forest canopy: measurements and modeling. Atmospheric Chemistry and Physics 7, 3361-3372.

Schade, G. W., Goldstein, A. H., 2001. Fluxes of oxygenated volatile organic compounds from a ponderosa pine plantation. Journal of Geophysical Research-Atmospheres 106, 3111-3123.

Steiner, A. H., Goldstein, A. L., 2007. Biogenic VOCs, in *Volatile organic compounds in the atmosphere*, (ed. Koppmann, R.), Wiley-Blackwell.

Taipale, R., Ruuskanen, T., Rinne, J., Kajos, M., Hakola, H., Pohja, T., Kulmala, M., 2008. Technical Note: Quantitative long-term measurements of VOC concentrations by PTR-MS - measurement, calibration, and volume mixing ratio calculation methods. Atmospheric Chemistry and Physics 8, 6681-6698.

Warneke, C., Karl, T., Judmaier, H., Hansel, A., Jordan, A., Lindinger, W., Crutzen, P. J., 1999. Acetone, methanol, and other partially oxidized volatile organic emissions from dead plant matter by abiological processes: Significance for atmospheric HOx chemistry. Global Biogeochemical Cycles 13, 9-17.

Tables

Table 1: Compounds measured during this study, with dwell times, sensitivities and limits of detection during the two halves of the measurement period.

m/z [amu]	Contributing compound(s)	Formula	Dwell time [s]	Sensitivity [ncps ppbv $^{-1}$]	Limit of detection [ppbv]	
					First half	Second half
21	water isotope	$H_2{}^{18}O$	0.2	-	-	-
33	methanol	CH_4O	0.5	9.53	0.58	0.95
37	water cluster	$(H_2O)_2$	0.2	-	-	-
45	acetaldehyde	C_2H_4O	0.5	11.1	0.21	0.27
59	acetone	C_3H_6O	0.5	10.1	0.10	0.11
	propanal					
60	trimethylamine (TMA)	$N(CH_3)_3$	0.5	8.25	0.09	0.13
69	isoprene	C_5H_8	0.5	2.42	0.24	0.26
	furan					
	methyl butenol fragment					
71	methyl vinyl ketone (MVK)	C_4H_6O	0.5	4.84	0.13	0.14
	methacrolein (MACR)					
81	monoterpene fragment (MT81)		0.5	1.9	0.36	0.28
83	(Z)-3-hexenol fragment		0.5	1.1	0.69	0.60
	(E)-3-hexenol fragment					
	(E)-2-hexenol fragment					
	hexanal fragment					
	(E,Z)-2-hexenyl acetate fragment					
87	2-methyl-3-buten-2-ol (MBO)	$C_5H_{10}O$	0.5	1	0.65	0.71
93	*p*-cymene fragment	C_7H_8	0.5	0.9	1.08	0.69
	toluene					
137	monoterpene (MT137)	$C_{10}H_{16}$	0.5	0.235	3.03	2.44
149	estragole	$C_{10}H_{12}O$	0.5	0.2	3.77	5.55

Table 2: Comparison of standardised emission rates of monoterpenes and isoprene from Douglas fir.

Species	Monoterpenes / µg g_{dw}^{-1} h^{-1}	Temperature coefficient / $°C^{-1}$	Isoprene / µg g_{dw}^{-1} h^{-1}	Measurement type	Reference
Pseudotsuga menziesii	0.8 ± 0.4 0.8 ± 0.3	0.19 ± 0.06 0.08 ± 0.05	0.09 ± 0.12 0.16 ± 0.18	Canopy-scale, PTR-MS	This study, first half This study, second half
"	0.44 ± 0.16	0.14 ± 0.05		Dynamic branch enclosure, mature forest	Pressley et al. (2004)
"	0.8 ± 0.2 (healthy) 6.8 (stressed)	0.133 ± 0.013 (healthy) 0.316 (stressed)		Dynamic branch enclosure, saplings	Joó et al. (2011)
"	1.81		<0.11	-	Guenther et al. (1994)
"	2.0		1.0	-	Karl et al. (2009)
"	2.3 ± 1.4		1.5 ± 1.6	-	Kesselmeir and Staudt (1999)
"	2.60 ± 1.63	assumed to be 0.09 ± 0.025	1.72 ± 1.85	Dynamic branch enclosure, mature trees	Drewitt et al. (1998)
Pseudotsuga macrocarpa	1.1 ± 0.3		0.0	Dynamic branch enclosure, immature tree (greenhouse)	Arey et al. (1995)

1

Figures

Figure 1: Average diurnal profiles of VOC fluxes above Douglas fir and of sensible heat flux, prior to 20:00 on 29th June 2009. Data points are the mean of median values for a ±1.5 hour time window. Note the variable scales. Grey areas show variability calculated as ±1 sd.

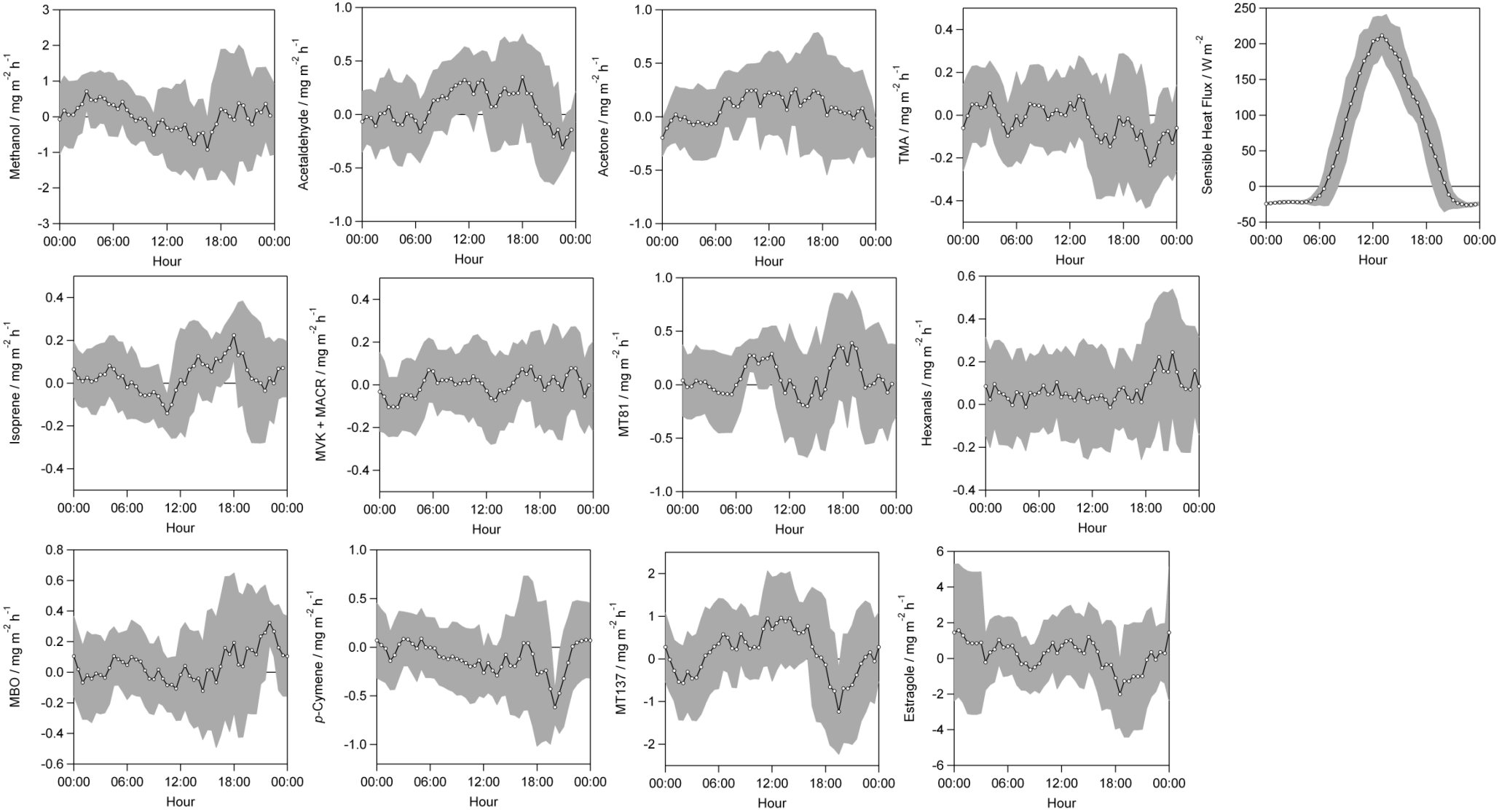

Figure 2: Average diurnal profiles of VOC mixing ratios above Douglas fir, and of temperature, before 20:00 on 29 June 2009. Note the variable scales. Dashed lines denote LOD. Grey areas show variability calculated as ±1 sd of the averaged half-hourly values of all measurements.

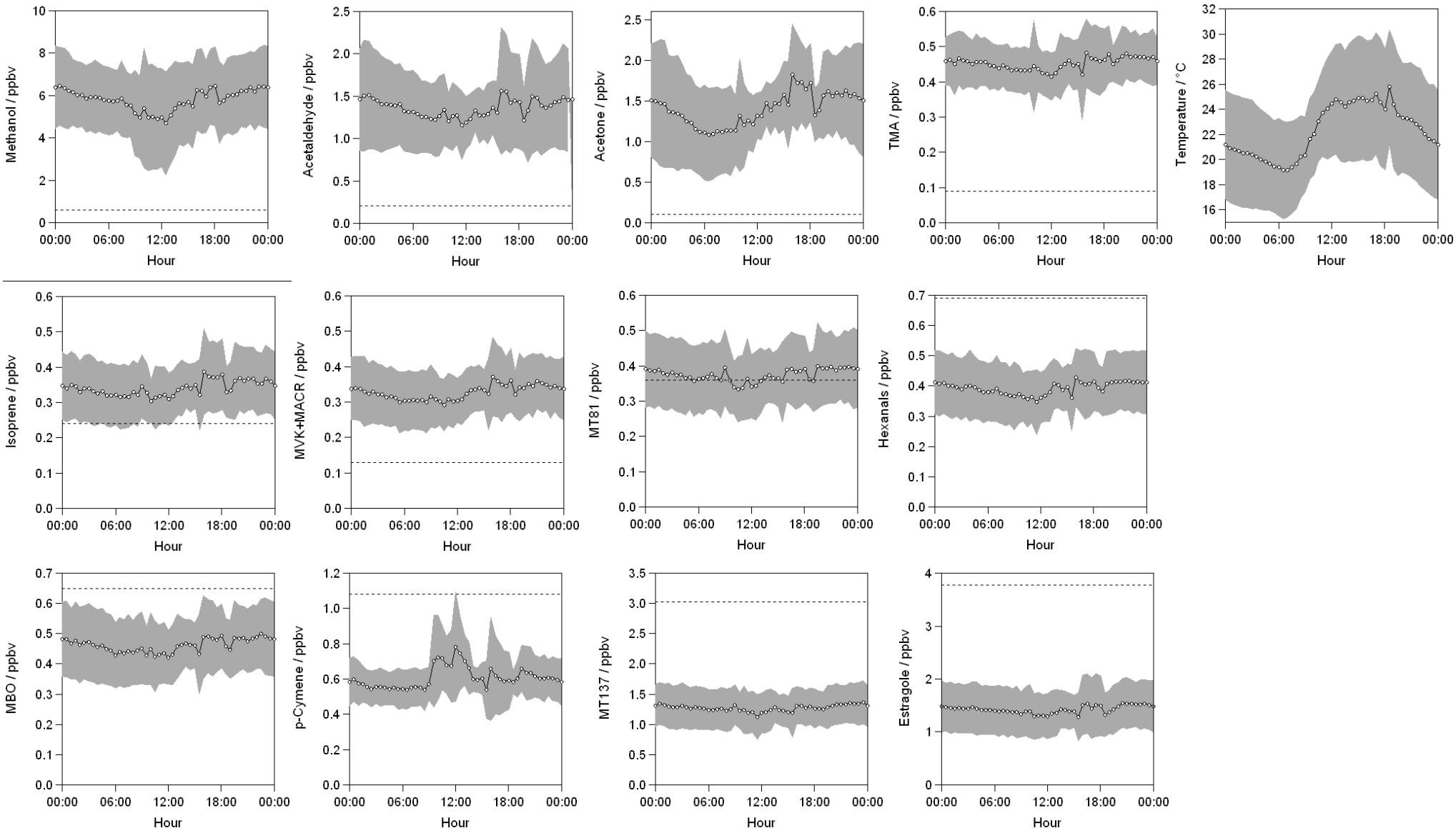

Figure 3: Within-canopy mixing ratios (ppbv, denoted by colour) as a function of time of day (hour, x-axis) and canopy height above ground (m, y-axis). Note the variable scales.

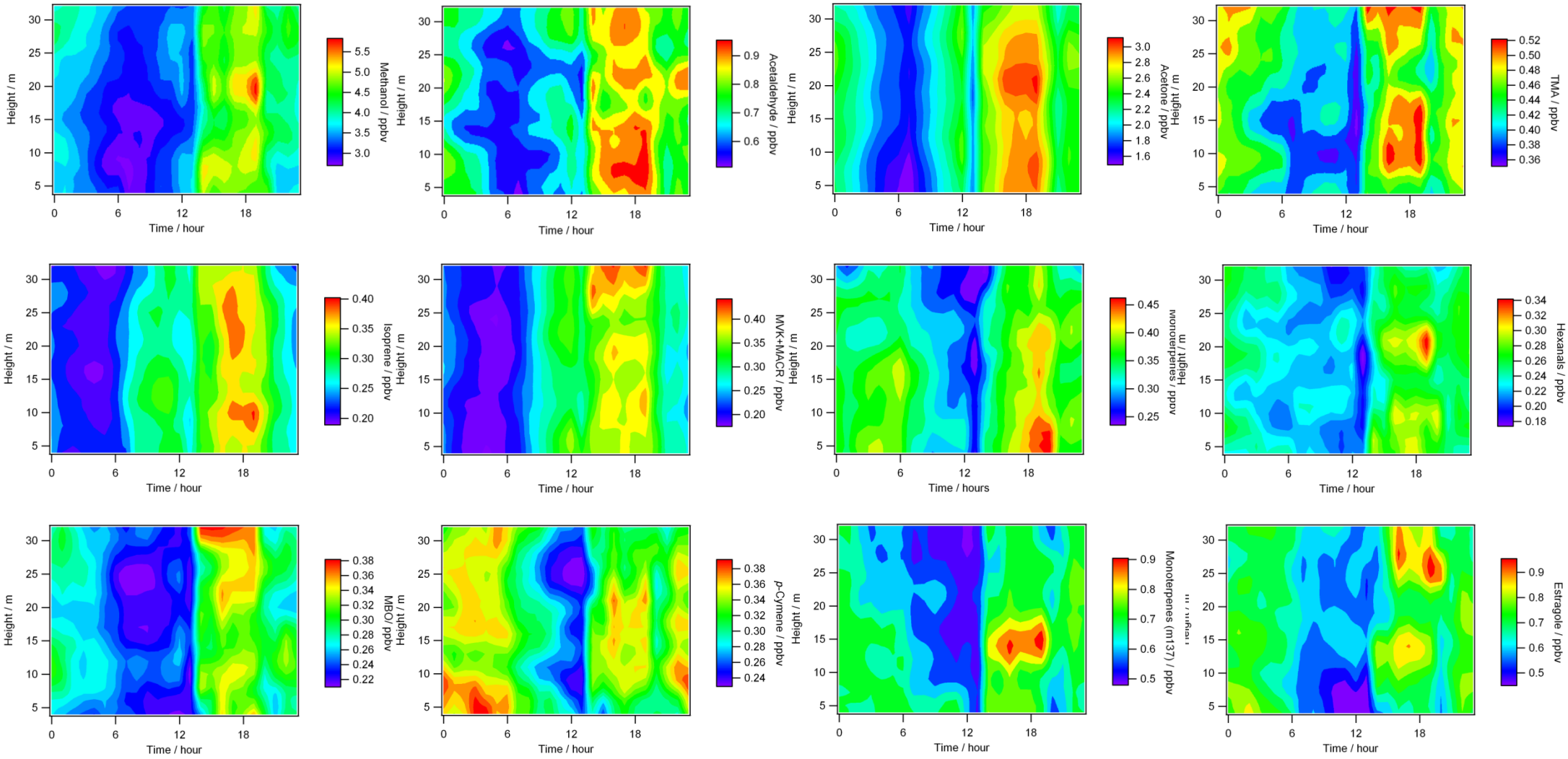

Supplementary Information

Volatile organic compound speciation above and within a Douglas Fir forest

Nichola Copeland[1,2], J. Neil Cape[1], Eiko Nemitz, Mathew R. Heal[2]

[1] Centre for Ecology & Hydrology, Bush Estate, Penicuik, EH26 0QB, UK

[2] EaStChem School of Chemistry, University of Edinburgh, West Mains Road, Edinburgh, EH9 3JJ, UK

Contents

Table S1: Atmospheric lifetimes of all compounds measured in this work.

Compound(s)		Atmospheric lifetimes		
		OH	O_3	NO_3
Methanol [a]		15 d		>220 d
Acetaldehyde [a]		11 h	>4.5 y	17 d
Acetone [a]		61 d	>4.5 y	>8 y
Trimethylamine (TMA) [b]		4.6 - 7 h	5.9 d	<53 d
Isoprene [a]		2 h	1.3 d	50 min
Methyl vinyl ketone (MVK) [a]		9 h	3.6 d	
Methacrolein (MACR) [a]		5 h	15 d	10 d
Monoterpenes	α-pinene [c]	2.6 h	4.6 h	11 min
	β-pinene [c]	1.8 h	1.1 d	27 min
	3-carene [c]	1.6 h	11 h	7 min
	limonene [c]	49 min	2 h	5 min
Hexanals [d]		7 h		
2-methyl-3-buten-2-ol (MBO) [e]		2.1 h		
p-Cymene [f]		1 d	>330 d	1.3 y
Estragole [g]		55 min	18 h	

[a] (Harrison and Hester, 1995), [OH] 1.6×10^6 cm^{-1}, [O_3] 7×10^{11} cm^{-1}, [NO_3] 5×10^8 cm^{-1}
[b] (Lee and Wexler, 2013), [OH] 1×10^6 cm^{-1}, [O_3] 2.5×10^{11} cm^{-1}, [NO_3] 5×10^8 cm^{-1}
[c] (Atkinson and Arey, 2003), [OH] 2×10^6 cm^{-1}, [O_3] 7×10^{11} cm^{-1}, [NO_3] 2.5×10^8 cm^{-1}
[d] (Jiménez et al., 2007), [OH] 1×10^6 cm^{-1}
[e] (Schade and Goldstein, 2001), [OH] 2×10^6 cm^{-1}
[f] (Corchnoy and Atkinson, 1990), [OH] 1.5×10^6 cm^{-1}, [O_3] 7×10^{11} cm^{-1}, [NO_3] 2.4×10^8 cm^{-1}
[g] (Bouvier-Brown et al., 2009), [OH] 5.4×10^6 cm^{-1}, [O_3] 1.18×10^{12} cm^{-1}

Figure S1: Location of the Speulderbos measurement site in The Netherlands superimposed on a land cover map. Adapted from Figure 7 in Clevers et al. (2007).

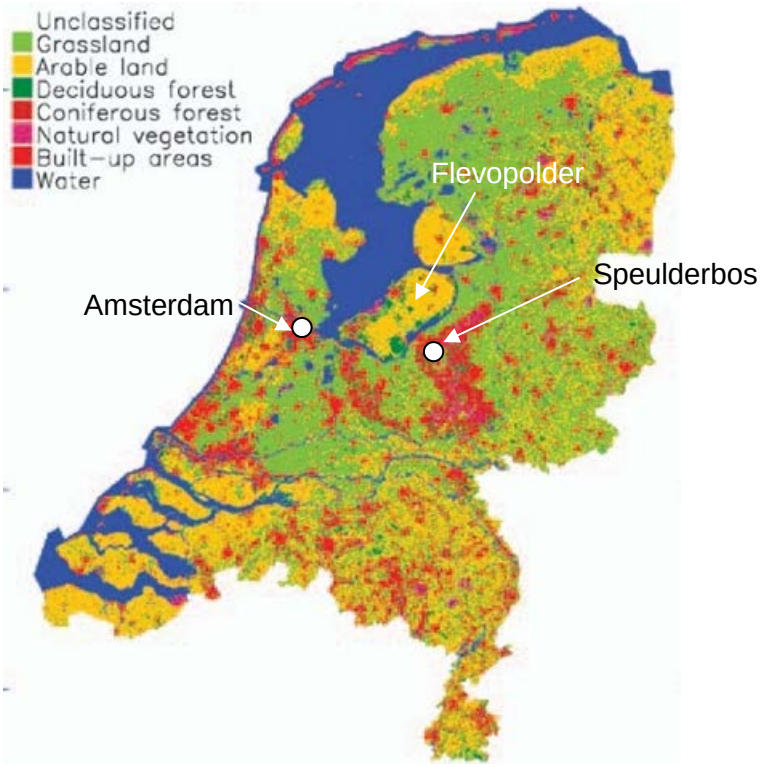

Figure S2: Aerial view of the Speuld measurement site. Grey lines show footpaths through the forest. The location of the sampling tower is indicated by the white marker. (Map attributable to ©2012 Aerodata International Surveys, Geoeye (Imagery) and ©2012 Google (map data)).

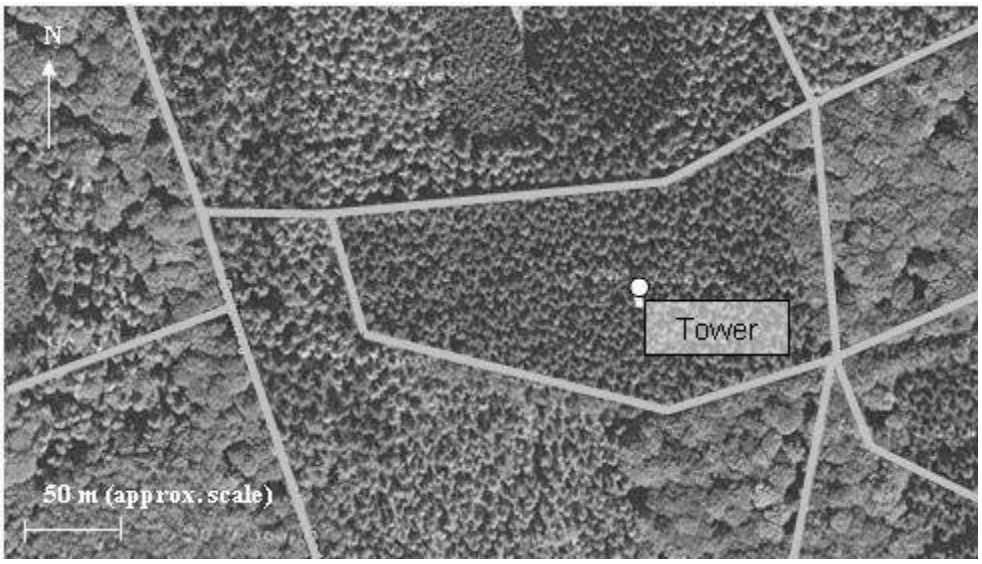

Figure S3: Modelled flux footprints for this study. The following parameters were used: measurement height z_m 45 m; roughness length z_0 3.2 m (estimated as 1/10th of the canopy height, 32 m); boundary layer height h 1000 m. Footprints were calculated for minimum, median and maximum values of u^* (1 sd of the vertical wind speed, σ_w, shown in brackets) as indicated on the graph. The distance at which maximum contribution can be expected, and at which 80% of the flux is contained, are given as X_{max} and X_r, respectively.

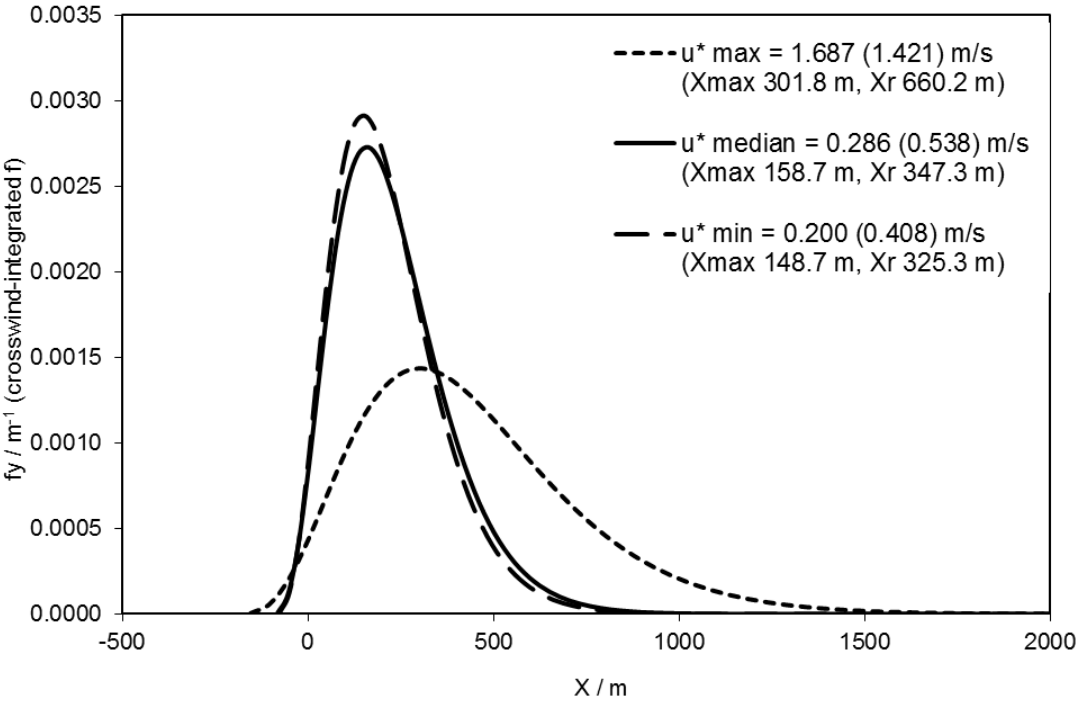

Figure S4: Map showing the predicted radius of the maximum 80% flux footprint using a simple parameterisation model (Kljun et al., 2004). The blue marker indicates the location of the sampling tower within Speuld forest. (Map data ©2012 Google Imagery ©2012 TerraMetrics. Radius plotted using www.freemaptools.com).

Figure S5: Time series of VOC fluxes measured above Douglas fir. Dashed gridlines denote midnight. Note the variable flux scales.

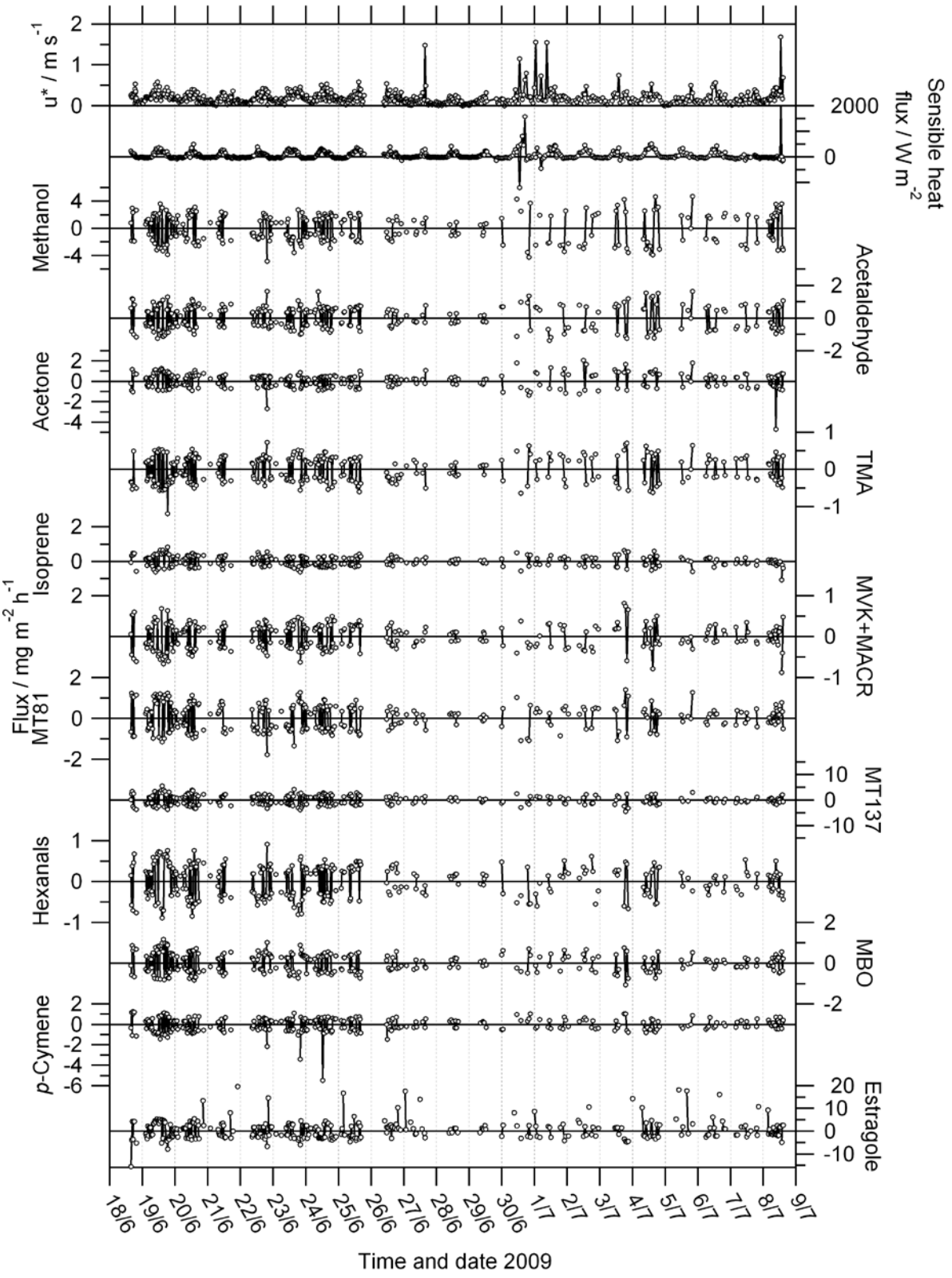

Figure S6: Average diurnal profiles of VOC fluxes above Douglas fir and of sensible heat flux, after 20:00 on 29 June 2009. Data points are the mean of median values for a ±1.5 hour time window. Note the variable scales. Grey areas show variability calculated as ±1 sd.

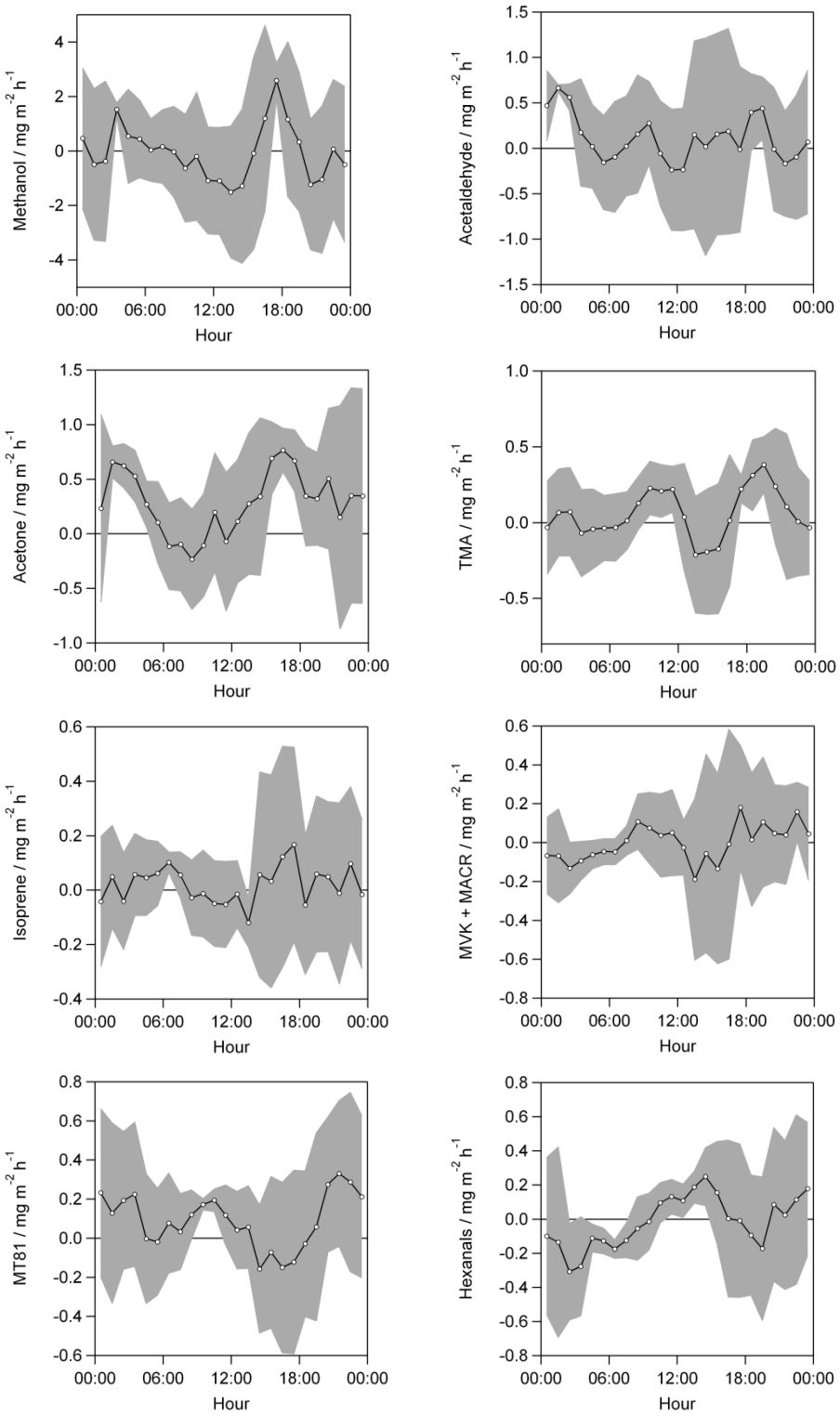

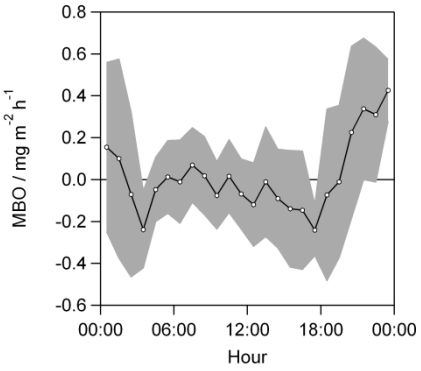
MBO / mg m-2 h-1
0.8
0.6
0.4
0.2
0.0
-0.2
-0.4
-0.6
00:00
06:00
12:00
18:00
00:00
Hour

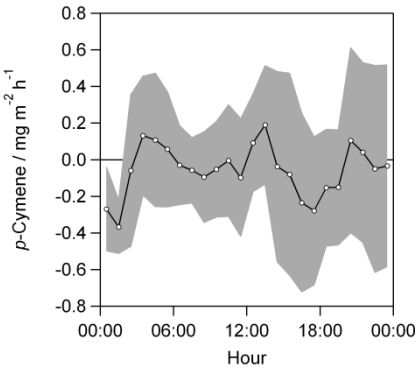
p-Cymene / mg m-2 h-1
0.8
0.6
0.4
0.2
0.0
-0.2
-0.4
-0.6
-0.8
00:00
06:00
12:00
18:00
00:00
Hour

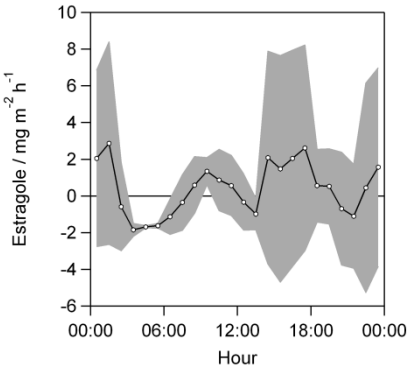
Estragole / mg m-2 h-1
10
8
6
4
2
0
-2
-4
-6
00:00
06:00
12:00
18:00
00:00
Hour

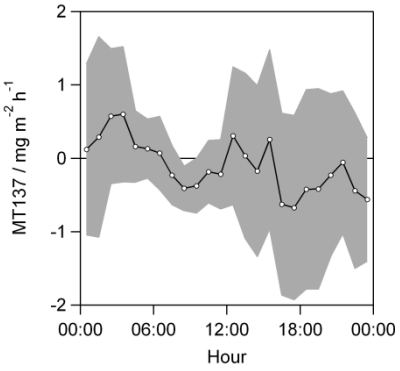
MT137 / mg m-2 h-1
2
1
0
-1
-2
00:00
06:00
12:00
18:00
00:00
Hour

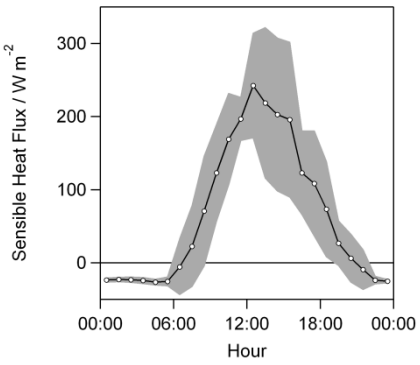
Sensible Heat Flux / W m-2
300
200
100
0
00:00
06:00
12:00
18:00
00:00
Hour

Figure S7: Time series of VOC mixing ratios, and of temperature, measured above Douglas fir. Dashed gridlines denote midnight. Note the variable mixing ratio scales.

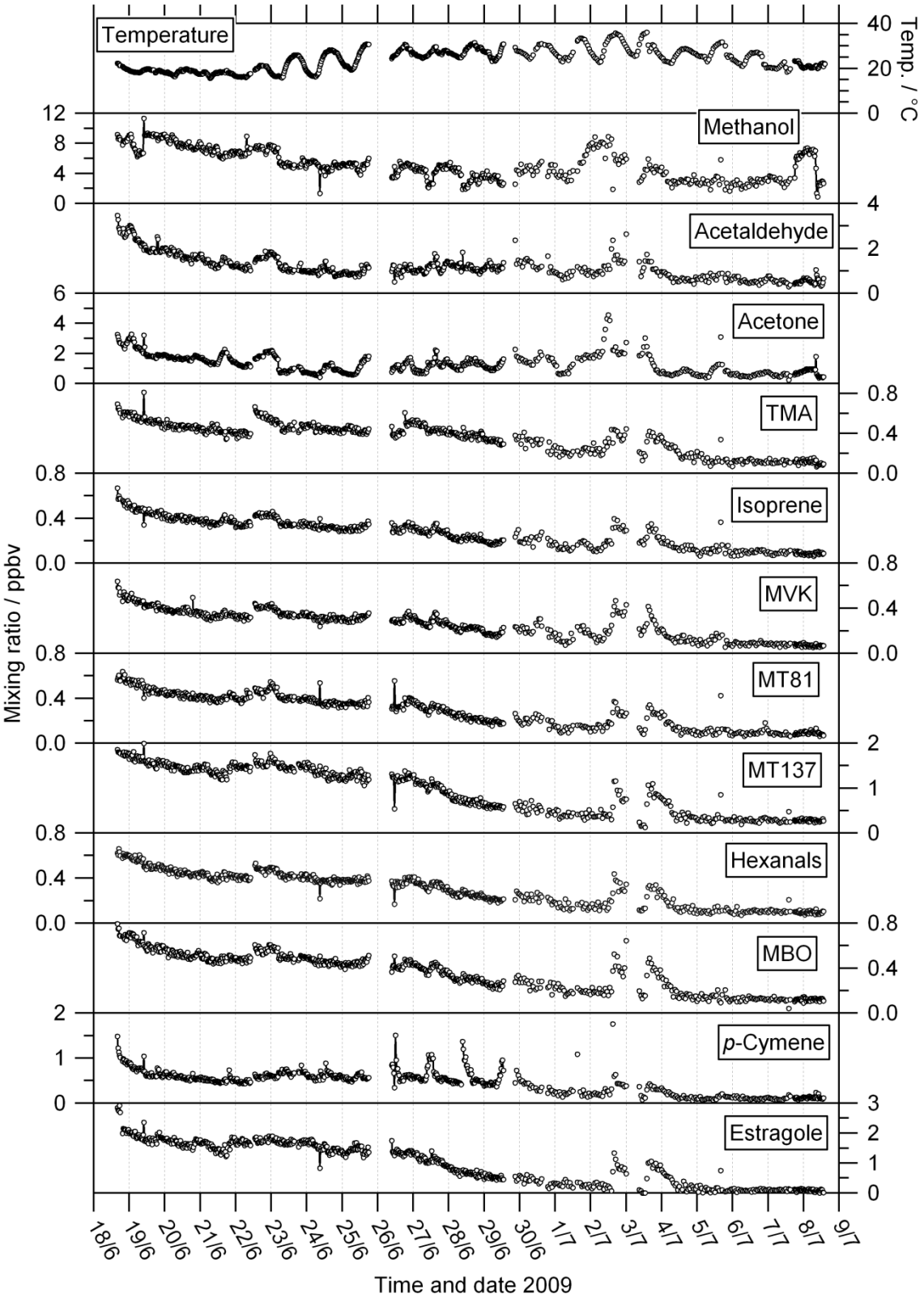

Figure S8: Average diurnal profiles of VOC mixing ratios above Douglas fir, and of temperature, after 20:00 on 29th June 2009. Note the variable scales. Dashed lines denote LOD. Grey areas show variability calculated as ±1 sd of the averaged half-hourly values of all measurements.

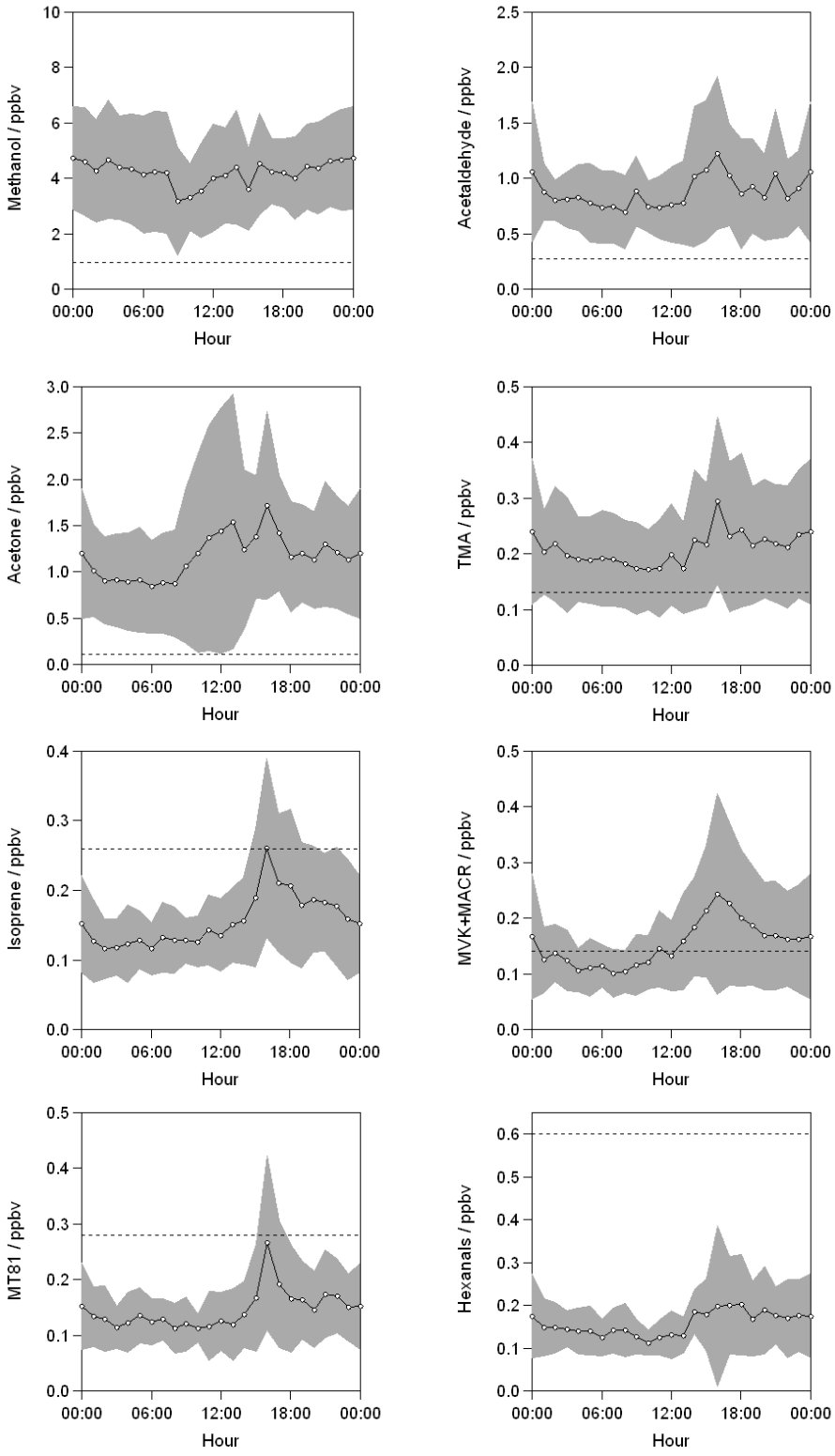

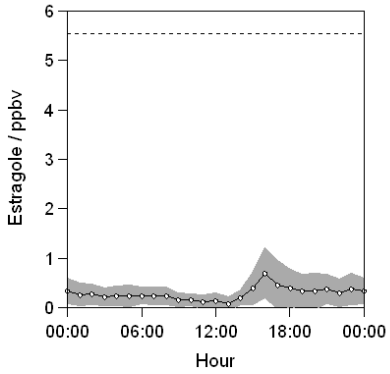
Estragole / ppbv
6
5
4
3
2
1
0
00:00
06:00
12:00
18:00
00:00
Hour

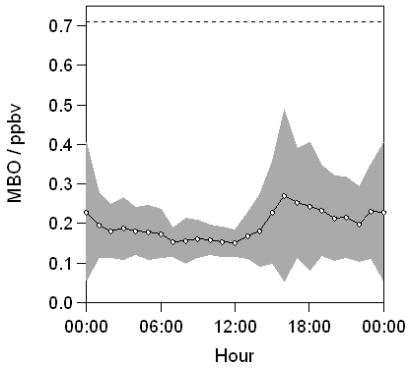
MBO / ppbv
0.7
0.6
0.5
0.4
0.3
0.2
0.1
0.0
00:00
06:00
12:00
18:00
00:00
Hour

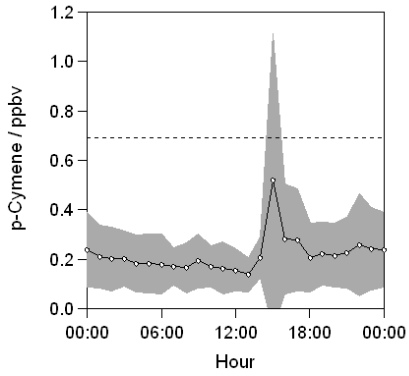
p-Cymene / ppbv
1.2
1.0
0.8
0.6
0.4
0.2
0.0
00:00
06:00
12:00
18:00
00:00
Hour

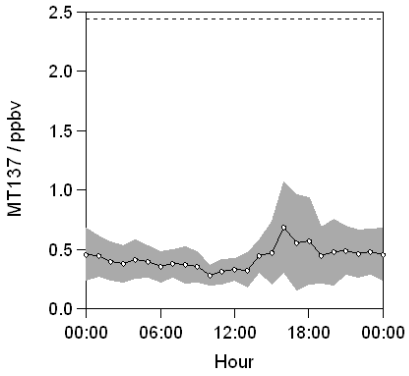
MT137 / ppbv
2.5
2.0
1.5
1.0
0.5
0.0
00:00
06:00
12:00
18:00
00:00
Hour

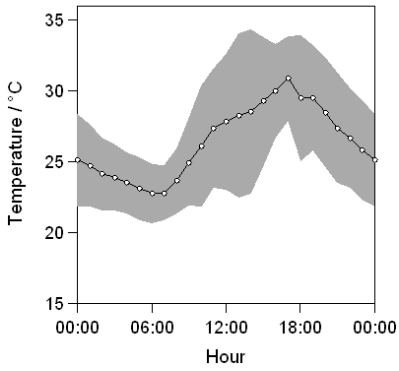
Temperature / °C
35
30
25
20
15
00:00
06:00
12:00
18:00
00:00
Hour

Figure S9: Bivariate plots of VOC mixing ratio by wind speed and wind direction. Polar coordinates correspond to wind direction, radial distance indicates wind speed (m s^{-1}) and colour denotes VOC mixing ratio according to the key for each individual plot. Temperature (°C) is shown for comparison.

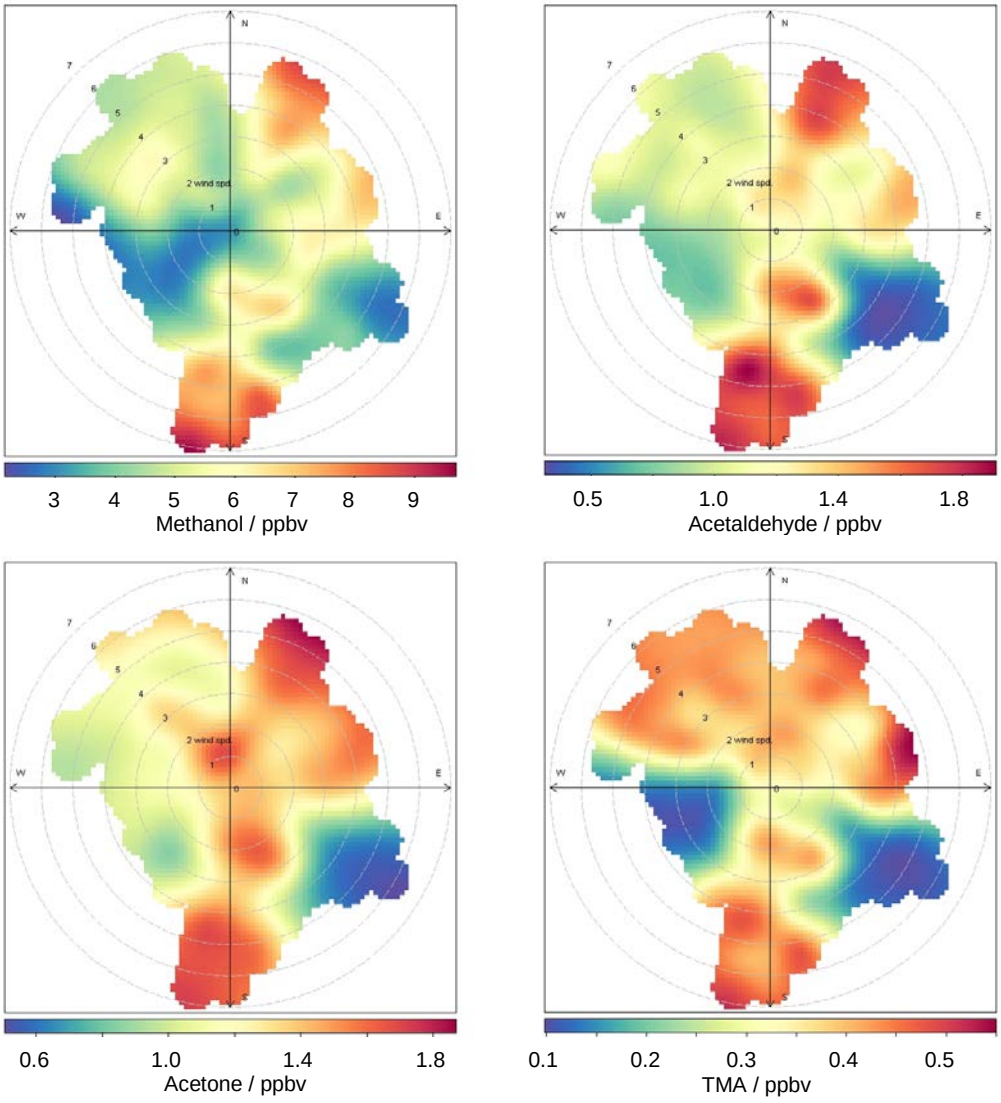

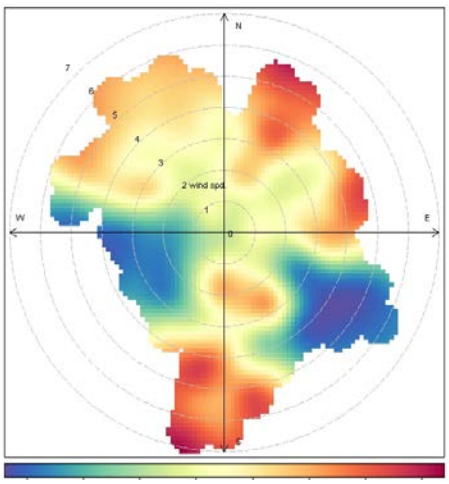

Isoprene / ppbv

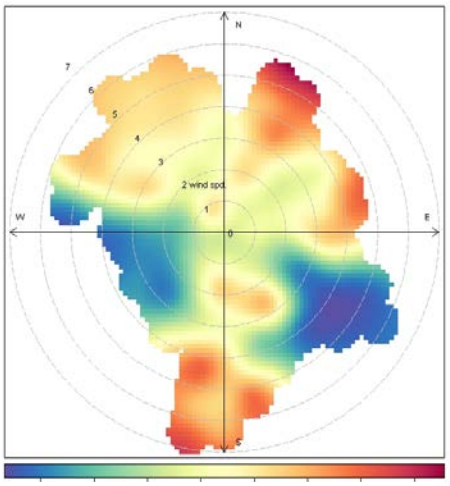

MVK+MACR / ppbv

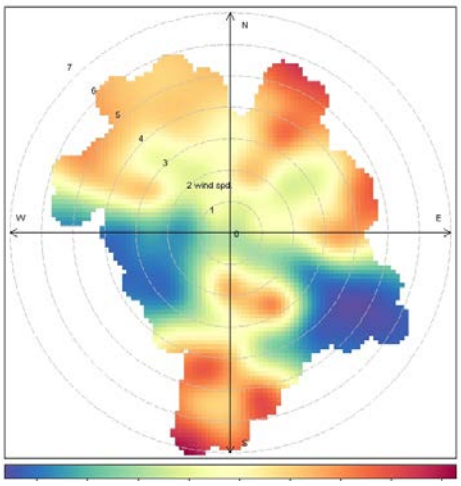

MT81 / ppbv

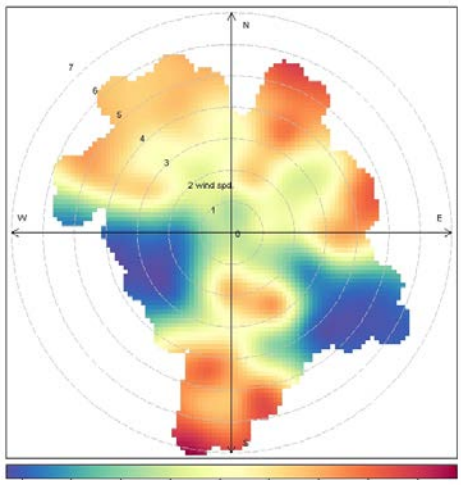

Hexanals / ppbv

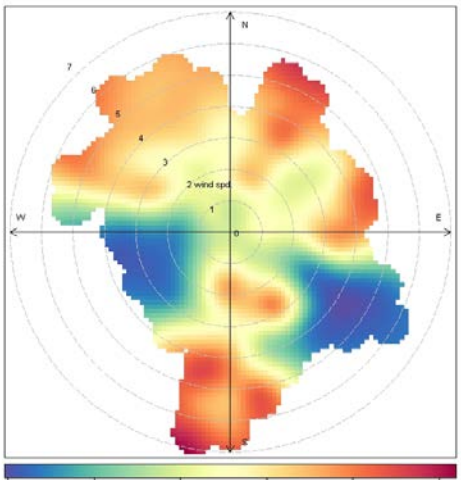

MBO / ppbv

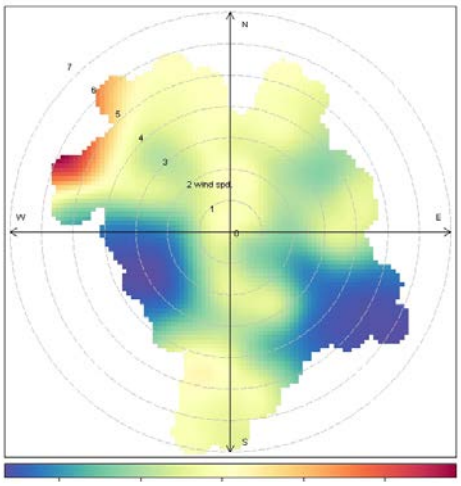

p-Cymene / ppbv

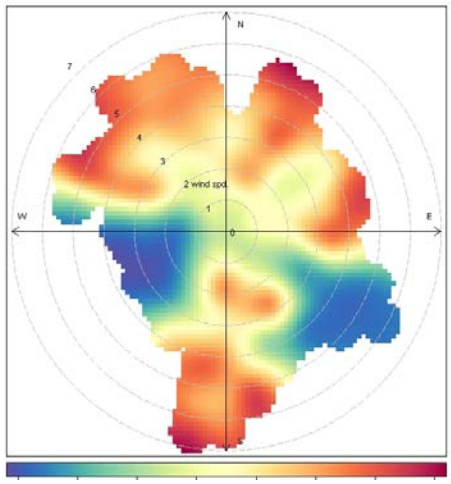
N
W
E
2 wind spd.
0.2
0.6
1.0
1.4
MT137 / ppbv

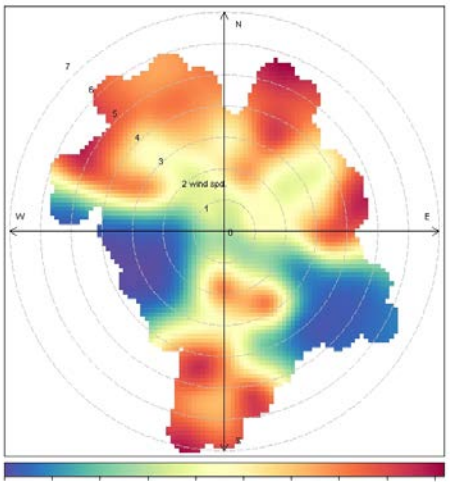
N
W
E
2 wind spd.
0
0.4
0.8
1.2
1.6
Estragole / ppbv

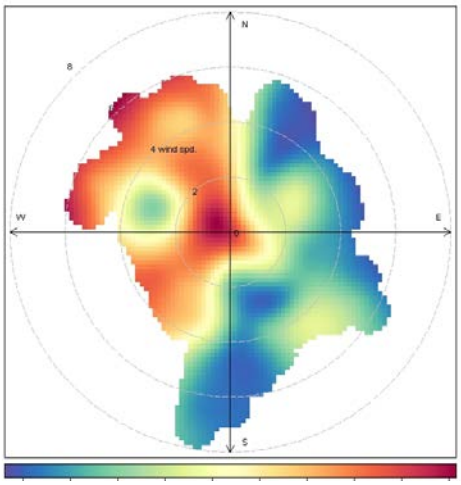
N
W
E
S
4 wind spd.
20
22
24
26
28
Temperature / °C

GC-MS analyses of ambient air samples

Methods

Ambient air samples were collected above the canopy (~40 m) approximately hourly from 08:10 to 20:08 on 6 July 2009 for subsequent GC-MS analysis. Samples were also taken at heights of 32, 18 and 4 m three times throughout the day (~09:30, 13:30 and 17:30) on 1 and 6 July 2009. A mass-flow controlled Pocket Pump (210-1000 Series, SKC Inc.) was used to pump air at 150 mL min^{-1} for 15 min through stainless steel adsorbent tubes (6 mm OD) packed with 200 mg Tenax TA and 100 mg CarboTrap (Markes International Ltd., UK). Prior to sampling, packed tubes had been conditioned at 300 °C for 15 min in a flow of He.

Analyses were undertaken using a Hewlett-Packard 5890/5970 GC-MS with an automated thermal desorption unit (ATD 400, Perkin Elmer) connected via a 200 °C heated transfer line. Transfer of samples from adsorbent tubes was performed in two steps: heat to 280 °C for 5 min at 25 mL min^{-1} to desorb samples onto a Tenax-TA cold trap at –30 °C, followed by transfer to the GC column at 300 °C for 6 min. Chromatographic separation utilised an Ultra-2 column (Agilent Technologies, 50 m × 0.2 mm ID × 0.11 µm film, 5% phenylmethyl silica) and temperature program of 35 °C for 2 min, heat at 5 °C min^{-1} to 160 °C, heat at 10 °C min^{-1} to 280 °C, and hold for 5 min.

A mixed monoterpene in methanol standard was prepared for calibration (10 ng μL^{-1} α-pinene, β-pinene, α-phellandrene, 3-carene and limonene (Sigma Aldrich, UK)). Aliquots of the standard (0, 1, 3 and 5 µL) were injected onto 4 adsorbent tubes with He carrier gas. Tubes continued to be purged with He for 2 min after injection. LODs for α-pinene and limonene were 0.23 and 0.30 ng on column, corresponding to mixing ratios of 18 and 24 pptv, respectively, for a 2.25 L sample. The GC-MS was subject to regular calibration: a set of standards was inserted between every 8 samples. Any intervening drift was accounted for. In addition, an extensive cross-check of PTR-MS and GC-MS calibration was carried out around this time, as described in the supplementary material of Misztal et al. (2011).

No in-line ozone scrubber was used, so it is acknowledged that there may have been uncharacterised losses of the reactive VOC from oxidation by ozone during the sampling and/or other on-tube interactions/rearrangements (Larsen et al., 1997; Helmig, 1997; Pollmann et al., 2005). The co-current collection of these samples (which occurred on 2 days out of the 4 week campaign) was only for the purposes of a spot inter-comparison against the

continuous PTR-MS data, and to provide an indication of speciation between α-pinene and β-pinene, which the PTR-MS cannot distinguish.

The rate coefficients between O_3 and the four terpenes determined by GC-MS – α-pinene, β-pinene, 3-carene and limonene – are, respectively, 9.4, 1.9, 4.8 and 21 × 10^{-17} cm^3 $molecule^{-1}$ s^{-1} at 298 K (http://iupac.pole-ether.fr). Based on simple first-order kinetics it is possible that during 1 h of sampling up to ~25% of α-pinene could be lost by reaction but only ~5% β-pinene. This yields an effective potential bias of ~20-25% in the GC-MS determination the α-pinene:β-pinene ratio, i.e. the GC-MS data underestimate this ratio. Limonene is a factor of two more reactive to O_3 than the other three detected terpenes; consequently the true relative proportion of limonene with respect to the pinenes may be underestimated. However, the relative trends diurnally and with height through the canopy for a given terpene should still be generally represented by the GC-MS data even if the absolute concentrations are in error.

Results and discussion

The above-canopy monoterpene mixing ratios determined by adsorption tube sampling and GC-MS analysis on one day are shown in Figure S10. Given the uncertainties in the GC-MS values, there is general consistency in the daily pattern and magnitude of mixing ratios for the pinenes between these measurements and those determined by PTR-MS (Figures 2 and S8). Mixing ratios for all monoterpenes in Figure S10 decreased during the morning, and were not detected between 13:00 and 18:00, but increased again in the early evening. α-Pinene had the highest mixing ratio throughout the day, followed by 3-carene and β-pinene. Since α-pinene may also have been subject to the greatest sampling loss of these three terpenes it is clear that α-pinene is the dominant of these three. Limonene was detectable in small amount only at 09:00, altough it is potentially subject to the greatest negative bias in sampling.

The average within-canopy total monoterpene mixing ratios determined by GC-MS are presented in Figure S11. These values compare fairly well with the in-canopy PTR-MS data (Figure 3). In-canopy (4 and 18 m) mixing ratios are highest in the morning and evening, and lowest in the afternoon, as was measured by PTR-MS. Conversely, peak mixing ratios measured in the afternoon were greater at the top of the canopy (32 m) and above (40 m). In general mixing ratios were larger at lower heights, again consistent with PTR-MS results.

The composition of total monoterpenes as a function of height through the canopy is illustrated in Figure S12. The data presented here are potentially subject to bias caused by the differntial losses of terpenes in sampling, as described above. α-Pinene is the dominant monoterpene at all heights (and its proportion may be underestimated relative to those of β-pinene and 3-carene) but its proportion of total monoterpenes decreases with height to a minimum at the canopy top (32 m) before increasing again above the canopy. The opposite vertical profile in contribution to total monoterpenes was observed for 3-carene whose contribution increased up to 32 m and decreased above canopy. The proportion of β-pinene decreased with height. Limonene made the lowest contribution to total monoterpenes with increasing contribution with canopy height (although its measurement is potentially subject to more negative bias than the other three terpenes). These results are consistent with a previous study at the Speuld site (Peters et al., 1994), and with another study which reported that α-pinene, β-pinene and 3-carene account for 95% monoterpene emissions from Douglas fir (Lerdau et al., 1995). This is reflected in Figure S12, except for measurements above the canopy (40 m) which may have been influenced by sources from the wider area.

Figure S10: Diurnal variation in monoterpene mixing ratios above the Douglas fir canopy (40 m). Samples were collected using adsorption tubes on 6 July 2009.

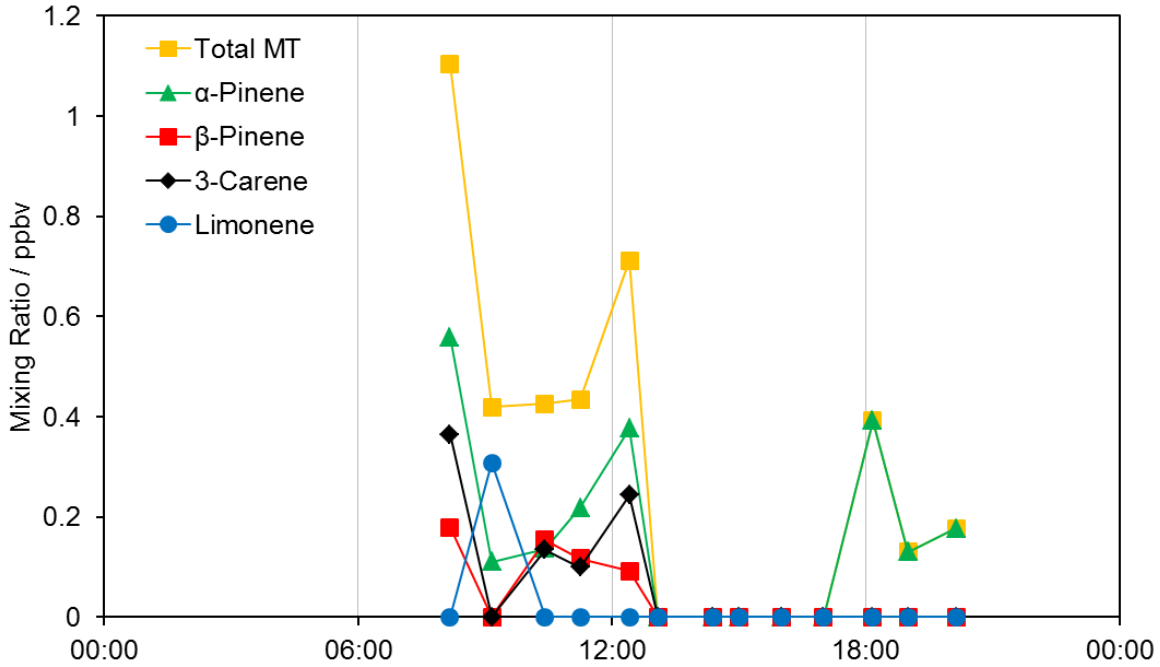

Figure S11: Average total monoterpene mixing ratios determined by GC-MS within the Douglas fir canopy. Samples were taken at three heights (4, 18 and 32 m) and at three times during the day (morning, afternoon, evening). Results shown are the averages of two sampling days (1 and 6 July) except for 40 m samples which were only taken on 6 July 2009.

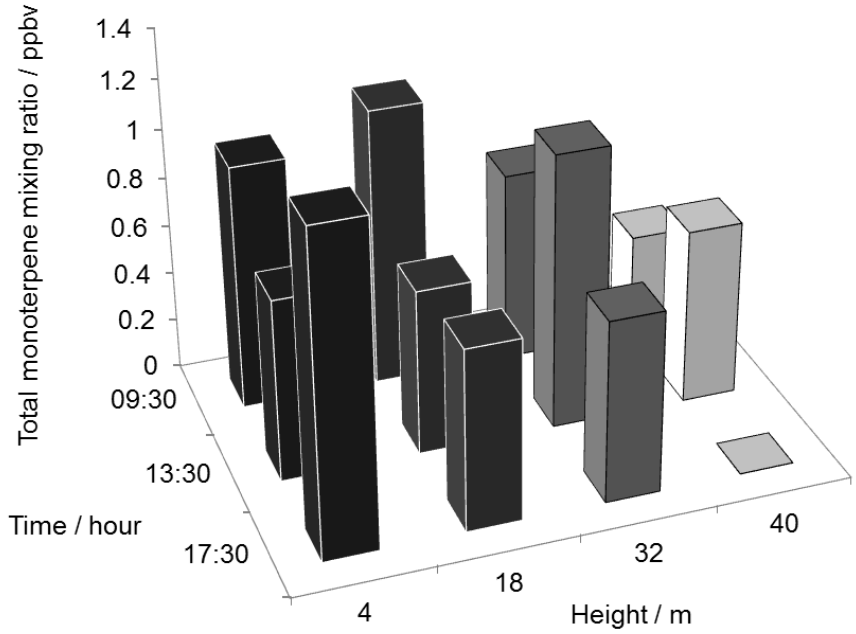

Figure S12: Monoterpene composition as a function of height above ground in the Douglas fir canopy. Each data point is a mean of 6 repeat measurements. Canopy top is at 32 m.

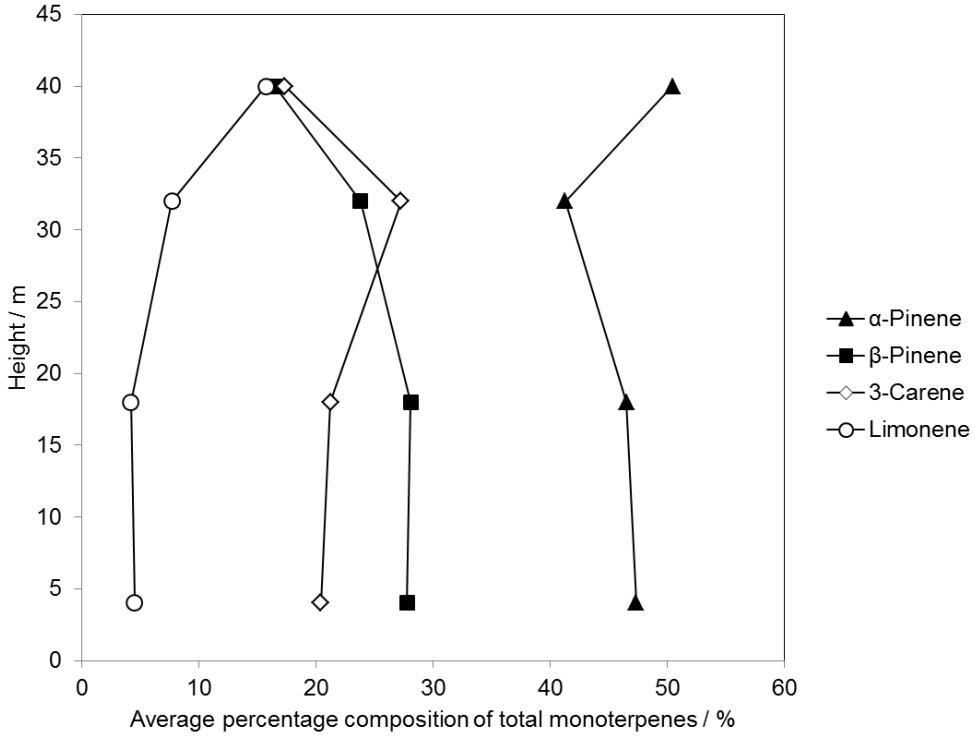

References

Atkinson, R., Arey, J., 2003. Gas-phase tropospheric chemistry of biogenic volatile organic compounds: a review. Atmospheric Environment 37, S197-S219.

Bouvier-Brown, N. C., Goldstein, A. H., Worton, D. R., Matross, D. M., Gilman, J. B., Kuster, W. C., Welsh-Bon, D., Warneke, C., de Gouw, J. A., Cahill, T. M., Holzinger, R., 2009. Methyl chavicol: characterization of its biogenic emission rate, abundance, and oxidation products in the atmosphere. Atmospheric Chemistry and Physics 9, 2061-2074.

Clevers, J., Schaepman, M., Mucher, C., De Wit, A., Zurita-Milla, R., Bartholomeus, H., 2007. Using MERIS on Envisat for land cover mapping in the Netherlands. International Journal of Remote Sensing 28, 637-652.

Corchnoy, S. B., Atkinson, R., 1990. Kinetics of the Gas-Phase Reactions of OH and NO3 Radicals with 2-Carene, 1,8-Cineole, Para-Cymene, and Terpinolene. Environmental Science & Technology 24, 1497-1502.

Harrison, R. M., Hester, R. E., 1995. *Volatile organic compounds in the atmosphere*, RSC, Cambridge.

Helmig, D., 1997. Ozone removal techniques in the sampling of atmospheric volatile organic trace gases. Atmospheric Environment 31, 3635-3651.

Jiménez, E., Lanza, B., Martinez, E., Albaladejo, J., 2007. Daytime tropospheric loss of hexanal and trans-2-hexenal: OH kinetics and UV photolysis. Atmospheric Chemistry and Physics 7, 1565-1574.

Larsen, B., Bomboi-Mingarro, T., Brancaleoni, E., et al , 1997. Sampling and analysis of terpenes in air. An interlaboratory comparison. Atmospheric Environment 31, 35-49.

Lee, D., Wexler, A. S., 2013. Atmospheric amines – Part III: Photochemistry and toxicity. Atmospheric Environment 71, 95-103.

Lerdau, M., Matson, P., Fall, R., Monson, R., 1995. Ecological Controls Over Monoterpene Emissions from Douglas-Fir (*Pseudotsuga-Menziesii*). Ecology 76, 2640-2647.

Misztal, P. K., Nemitz, E., Langford, B., Di Marco, C. F., Phillips, G. J., Hewitt, C. N., MacKenzie, A. R., Owen, S. M., Fowler, D., Heal, M. R., Cape, J. N., 2011. Direct ecosystem fluxes of volatile organic compounds from oil palms in South-East Asia. Atmospheric Chemistry and Physics 11, 8995-9017.

Peters, R. J. B., Duivenbode, J. A. D. V., Duyzer, J. H., Verhagen, H. L. M., 1994. The determination of terpenes in foreset air. Atmospheric Environment 28, 2413-2419.

Pollmann, J., Ortega, J., Helmig, D., 2005. Analysis of atmospheric sesquiterpenes: Sampling losses and mitigation of ozone interferences. Environmental Science & Technology 39, 9620-9629.

Schade, G. W., Goldstein, A. H., 2001. Fluxes of oxygenated volatile organic compounds from a ponderosa pine plantation. Journal of Geophysical Research-Atmospheres 106, 3111-3123.